



Boletín de la Sociedad Geológica
Mexicana

ISSN: 1405-3322

sgm_editorial@geociencias.unam.mx

Sociedad Geológica Mexicana, A.C.
México

Piñán-Llamas, Aránzazu; Escamilla-Casas, José C.
Provenance and tectonic setting of Neoproterozoic to Early Cambrian metasedimentary
rocks from the Cordillera Oriental and Eastern Sierras Pampeanas, NW Argentina
Boletín de la Sociedad Geológica Mexicana, vol. 65, núm. 2, 2013, pp. 373-395
Sociedad Geológica Mexicana, A.C.
Distrito Federal, México

Available in: <http://www.redalyc.org/articulo.oa?id=94348266019>

- How to cite
- Complete issue
- More information about this article
- Journal's homepage in redalyc.org

redalyc.org

Scientific Information System

Network of Scientific Journals from Latin America, the Caribbean, Spain and Portugal

Non-profit academic project, developed under the open access initiative



Provenance and tectonic setting of Neoproterozoic to Early Cambrian metasedimentary rocks from the Cordillera Oriental and Eastern Sierras Pampeanas, NW Argentina

Aránzazu Piñán-Llamas^{1,*}, José C. Escamilla-Casas²

¹ Indiana University-Purdue University Fort Wayne, 2101 E. Coliseum Blvd. Fort Wayne, IN 46805. Phone: (260) 481-6253.

² Universidad Autónoma del Estado de Hidalgo. Área Académica de Ciencias de la Tierra y Materiales. Ciudad Universitaria Carretera Pachuca – Tulancingo Km. 4.5 C.P. 42184. Col. Carboneras, Mineral de la Reforma, Hidalgo. Phone: 0177171 72000.

* pinana@ipfw.edu

Abstract

Major, trace, and rare-earth element data for the Neoproterozoic to early Cambrian Puncoviscana Formation and related higher-grade metasedimentary rocks in Eastern Sierras Pampeanas, NW Argentina, were analyzed to evaluate their provenance, weathering, and tectonic setting during the upper Neoproterozoic-lower Paleozoic. The studied rocks are metapelites and metapsammites that were mainly affected by the lower Cambrian Pampean orogeny. Geochemical analyses indicate that the Puncoviscana Fm. and related rocks are characterized by moderate Chemical Index of Alteration (CIA) values. REE element distributions, Eu/Eu* values, and high Zr/Sc and Th/Sc ratios indicate that the samples were likely derived from predominantly upper-crust felsic sources. Tectonic discrimination diagrams based on immobile trace elements (e.g. Th-La-Sc, Sc-Th-Zr/10), multi-element patterns, REE characteristics, and diagnostic trace element ratios (i.e. Th/Sc, Zr/Hf, La/Th, La/Sc) imply that the tectonic setting of the source area was a continental island arc and/or an active continental margin. Geochemical signatures of low-grade metapsammitic samples (high Hf and Zr content, and high Zr/Sc ratios) indicate crustal recycling.

The geometry and sequence of structures and microstructures preserved in all samples are pervasive and suggest a common and uniform deformational history during the Pampean orogeny. Geochemical signatures and structures of the studied samples are consistent with protolithic sediments of the Puncoviscana Fm. and related rocks initially deposited in an arc-related basin that was subsequently deformed during the Pampean orogeny.

Keywords: Geochemistry, metasedimentary rocks, provenance, Pampean orogeny, Puncoviscana Formation.

Resumen

En este estudio, se caracteriza la proveniencia, grado de alteración, y el ambiente tectónico de rocas metasedimentarias de edad Neoproterozoica a Cámbrico Temprano del NW de Argentina, (Formación Puncoviscana y rocas equivalentes de mayor grado metamórfico aflorantes en las Sierras Pampeanas Orientales) durante el Neoproterozoico superior al Paleozoico inferior, en base al análisis de datos de elementos mayores, trazas, y tierras raras. Las rocas analizadas son metapelitas y metapsamitas que fueron afectadas principalmente por la orogenia Pampeana (Cámbrico Inferior). Los resultados geoquímicos indican que estas rocas se caracterizan por presentar valores moderados en el Índice Químico de Alteración (CIA). Las distribución de tierras raras, y los valores de Eu/Eu, Zr/Sc, y Th/Sc indican que las muestras se derivaron muy probablemente y de forma predominante, de rocas fuente félsicas de la corteza superior. Diagramas de discriminación tectónica basados en elementos traza inmóviles (e.g. Th-La-Sc, Sc-Th-Zr/10), patrones multielementos, características de las tierras raras y relaciones de elementos traza útiles en la discriminación del ambiente tectónico (i.e. Th/Sc, Zr/Hf, La/Th, La/Sc) indican que el ambiente tectónico del área fuente pudo ser un arco de islas continental y/o*

un margen activo continental. La signatura geoquímica de las metapsamitas de bajo grado (que incluye altos contenidos de Hf y Zr y valores altos de Zr/Sc), indica la presencia de una componente sedimentaria de reciclado cortical en estas rocas.

La geometría y secuencia de estructuras y microestructuras preservadas en la totalidad de las muestras estudiadas, sugieren que estas rocas comparten una historia de deformación común y uniforme durante la orogenia Pampeana. Tanto las signaturas geoquímicas como las estructuras de las rocas estudiadas indican que los protolitos sedimentarios de la Formación Puncoviscana y rocas asociadas se depositaron en una cuenca relacionada con un arco volcánico que, subsecuentemente, fue deformada durante la orogenia Pampeana.

Palabras Clave: Geoquímica, rocas metasedimentarias, proveniencia, orogenia Pampeana, Formación Puncoviscana.

1. Introduction

The Ediacaran-Early Cambrian Puncoviscana Formation (Turner, 1960; Figure 1a), a thick turbiditic sequence exposed in the Puna and Cordillera Oriental and a series of metaclastic successions in Eastern Sierras Pampeanas, considered as its higher-grade equivalents (Willner and Miller, 1985; Rapela *et al.*, 1998; Schwartz and Gromet, 2004), were initially deposited on the western margin of Gondwana during the Neoproterozoic to lower Cambrian and deformed and metamorphosed during the lower Cambrian Pampean orogeny (Rapela *et al.*, 2002; Siegesmund *et al.*, 2010; Escayola *et al.*, 2011). The study of the geological evolution of the Puncoviscana Fm. and related rocks is critical to understand the Pampean orogeny and the early geodynamic evolution of the western Gondwana margin. We investigate the geochemical signature of these rocks in order to constrain their provenance and depositional tectonic setting, and to discuss their evolution during the Neoproterozoic-early Paleozoic. Previous provenance studies have been carried out in the region resulting in different interpretations and tectonic models (Do Campo and Ribeiro-Guevara, 2002, 2005; Zimmermann, 2005; Rapela *et al.*, 2007; Collo *et al.*, 2009; Drobe *et al.*, 2011; Hauser *et al.*, 2011). Thus, the depositional setting and tectonic evolution of the Puncoviscana metasedimentary rocks and related rocks during the lower Paleozoic is still under debate.

Geochemistry has been traditionally used to determine the provenance of clastic and metaclastic rocks and to constrain the tectonic setting in which they were deposited (e.g. McLennan *et al.*, 1983, 1990, 1993, 1995; Taylor and McLennan, 1985, 1995; Bhatia and Crook, 1986; Roser and Korsch, 1985, 1988; Gu, 1996a, 1996b). Petrographic analyses based on framework modes are usually less useful than geochemical analyses in the characterization of provenance and tectonic setting of metamorphic rocks if the samples contain considerable amounts of pseudo matrix. The transformation of labile fragments originally present in the rock (*i.e.* feldspar or rock fragments) into clay minerals (pseudo matrix) can bias framework modes toward the quartz apices of classification diagrams (Do Campo and Ribeiro-Guevara, 2005). Furthermore, the geochemistry of metasediments is particularly valuable in the study of fine-grained rocks that are difficult to characterize through

petrographic studies.

Major and trace elements can constraint the effects of weathering and sedimentary sorting, while rare earth and certain trace elements (e.g. Th, Zr, Hf, Nb, and Sc) are considered particularly reliable in the discrimination of provenance and tectonic setting. This reliability is based on their low mobility during sedimentary processes, diagenesis, and metamorphism, thus reflecting the signature of the parent materials, and the composition and tectonic environment of the source (Taylor and McLennan, 1985; McLennan, 1989; McLennan *et al.*, 1993; Roser *et al.*, 1996; Condie, 1991, 1993). Provenance studies of medium and high metamorphic grade metasediments are relatively common in the literature (*i.e.* Li *et al.*, 2005; Meinhold *et al.*, 2007; Drobe *et al.*, 2011; Verdecchia and Baldo, 2010).

In this paper, we present new major and trace element whole-rock geochemical analyses from the Puncoviscana Fm. and related metasedimentary rocks from Cumbres Calchaquies, Sierras de Quilmes, Ancasti, and Córdoba (Figure 1). We combine our results with previously published data (Willner *et al.*, 1985; Do Campo and Ribeiro-Guevara, 2005; Zimmermann, 2005) to evaluate their source and tectonic depositional setting. The characterization of the provenance and tectonic setting of these units is important for understanding the geodynamic evolution of the western Gondwana margin during the early Paleozoic. We also present new structural and microstructural data to support the correlation of our samples along the orogen during the Pampean cycle.

2. Tectonic setting

The Eastern Sierras Pampeanas are isolated basement blocks exhumed as a result of Tertiary to recent high-angle reverse faulting (Jordan and Allmendinger, 1986) associated with the flat slab subduction of the Nazca Plate (Ramos *et al.*, 2002). These blocks include large outcrops of metaclastic rocks that extend between 26° and 33° S (Figure 1), and were mainly affected by lower Cambrian deformation, metamorphism, and magmatism (the Pampean orogeny; e.g. Rapela *et al.*, 1998, 2002; Siegesmund *et al.*, 2010; Escayola *et al.*, 2011). Based on isotope studies (e.g. Schwartz and Gromet, 2004; Steenken *et al.*, 2004; Drobe *et al.*, 2009 and

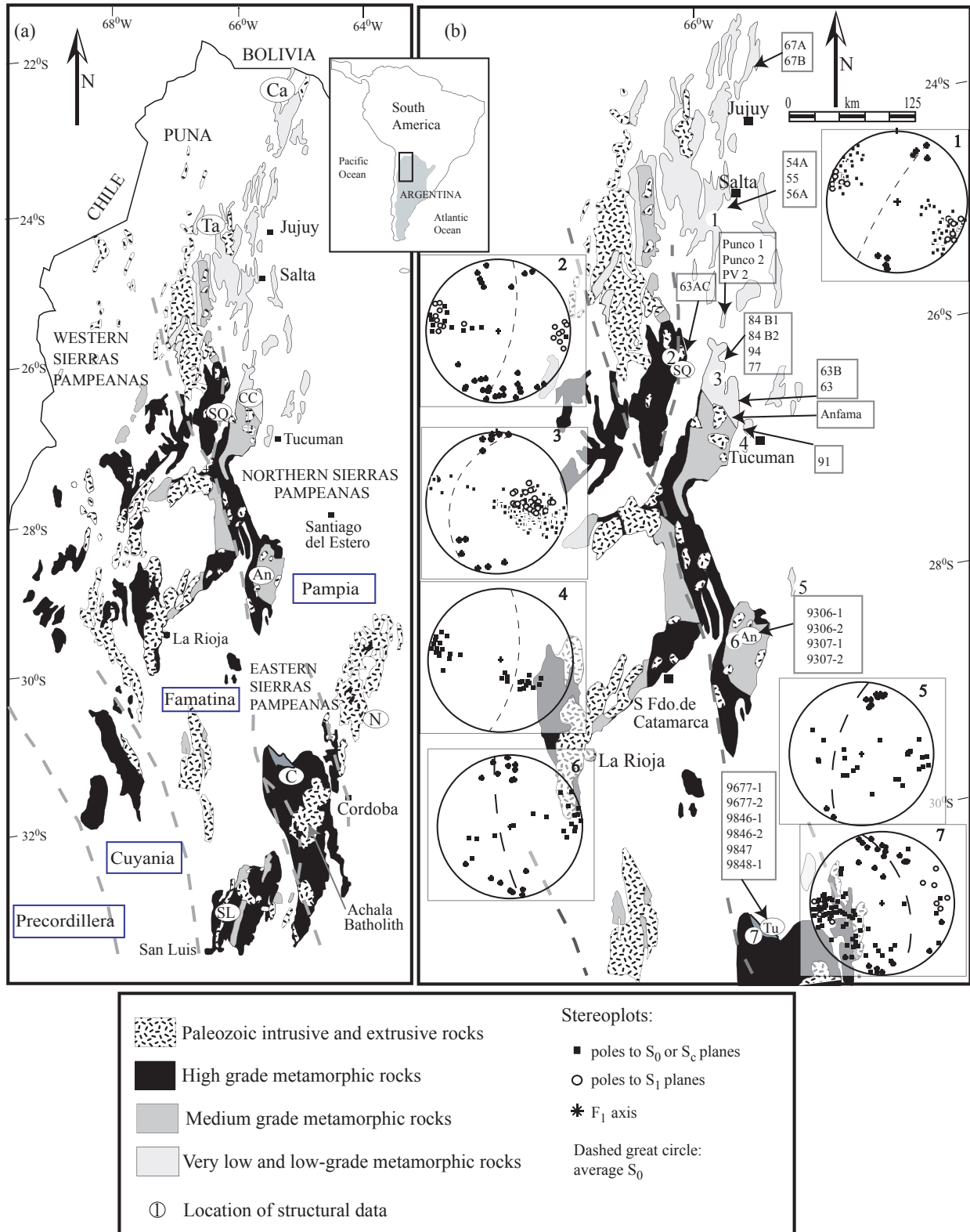


Figure 1. (a) Simplified geological map of lower Paleozoic rocks in NW Argentina, modified from Willner and Miller (1985), and Simpson *et al.* (2003). Inset shows the location of the research area in Argentina (boxed). Dashed lines indicate approximate boundaries between peri-Gondwanan terranes. (b) Puncoviscana Fm. and higher-grade related rocks with location of samples and structural data plotted on lower hemisphere stereographic projections. Number of structural data (stereoplot number here between parentheses): Salta (1) S_0 n=52, S_1 n=13, F_1 axes n=8; Quilmes (2) S_0 n=12, S_1 n=17, F_1 axes n=29; Hualinchay (3) S_0 n=71, S_1 n=22, F_1 axes n=12; Sierra de San Javier (4) S_0 n=31; Guasayan (5) S_0 n=25, F_1 axes n=12; Ancasti (6) S_0 n=19, F_1 axes n=17; Tuclame (7) S_0 n=61, S_1 n=10, F_1 axes n=21. Paleozoic mountain ranges and localities mentioned in the text: Tu. Tuclame; An. Ancasti; CC. Cumbres Calchaquies; C. Córdoba; SL. San Luis; N. Sierra del Norte; Ta. Sta. Rosa de Tástil; Ca. Cañaní; SQ Sierra de Quilmes.

references therein) these rocks have been correlated with the Ediacaran to Early Cambrian Puncoviscana Formation (Turner, 1960) that crops out along a NNE-SSW linear belt that extends from the Bolivian border (22°S) to the vicinity of Salta (~26°S; Figure 1a). Protoliths of the very low- to low-grade Puncoviscana Fm. and the medium- to high-grade metaclastic rocks of the Eastern Sierras Pampeanas have been interpreted by several authors as deposited in the same basin (Puncoviscana Basin) that extended from Bolivia to central Argentina (~33°S) roughly between 64°W and 68°W (Jezek, 1990; Rapela *et al.*, 1990; Figure 1 of Zimmermann, 2005). However, the unexposed contact between low-grade and medium- to high-grade units, the discontinuity between outcrops, and the lack of a reliable stratigraphic column complicate the interpretation of the paleotectonism of the basin. Mon and Hongn (1991) subdivided the Pampean basement between 22°S to 28°S into several orogenic belts with a different tectonometamorphic evolution and suggest that higher-grade rocks are older than the Puncoviscana Fm.

The Puncoviscana Fm. includes successions of metamorphosed greywackes, siltstones, and mudstones, and locally interbedded metaconglomerates and discontinuous marble lenses (Jezek, 1990; Omarini *et al.*, 1999; Porto *et al.*, 1990); it also preserves sedimentary structures, and fossils of Ediacaran to Early Cambrian age (Aceñolaza and Durand, 1986; Durand, 1996). Sedimentological and facies analyses indicate a unidirectional pattern of sediment transport from east to west/northwest (present-day coordinates) from a common source area (Jezek *et al.*, 1985; Jezek, 1990). Geochemical signatures of alkaline lava flows, sills, and basic dikes in the turbiditic section indicate oceanic-island to within-plate settings (Coira and Barber, 1987; Coira *et al.*, 1990) consistent with a rift environment. Based on geochemical signatures obtained from basalts of uncertain stratigraphic position that are interbedded in metaclastic rocks of the Puncoviscana Fm., Omarini *et al.* (1999) suggest a transition from rift to a back-arc environment.

Idiomorphic detrital zircons from volcanoclastic beds in mid and upper stratigraphic levels of the Puncoviscana Fm. yielded an age range of 530–560 Ma (U-Pb, Lork *et al.*, 1990), considered as a maximum sedimentation age. Adams *et al.*, 2008a, 2008b reported maximum sedimentation ages of 636 ± 7 – 551 ± 5 Ma. More recently, Escayola *et al.* (2011) obtained ages of 536.4 ± 5.3 Ma and 537 ± 0.9 Ma from tuffaceous beds interlayered with metaclastic rocks of the Puncoviscana Fm. Detrital zircons from Puncoviscana Fm. rocks in the Cordillera Oriental yielded late Mesoproterozoic to early Neoproterozoic (850–1150 Ma), and late Neoproterozoic–Early Cambrian (650–520 Ma) U-Pb age maxima (Adams *et al.*, 2011). A similar age distribution of detrital zircon population was obtained by Escayola *et al.* (2011) and Hauser *et al.* (2011), but these authors describe much stronger late Ediacaran peaks suggesting that deposition of the Puncoviscana Fm. likely started in the latest Ediacaran but is mainly Early Cambrian,

and was coeval with a nearby magmatic arc (Escayola *et al.*, 2011). The depositional age of the Puncoviscana Fm. is additionally constrained by the unconformably overlying shallow marine platform metasedimentary rocks of the Meson Group that contain poorly preserved middle to Late Cambrian trilobites (Sánchez and Salfity, 1999; Aceñolaza *et al.*, 2002; Aceñolaza and Aceñolaza 2005). Based on U-Pb geochronology of detrital zircons, and the pre-depositional Santa Rosa de Tastil batholith, Augustsson *et al.* (2011) suggest a mainly middle Cambrian depositional age for the Meson Group. Adams *et al.* (2011) report a youngest zircon component at 500 Ma, suggesting an upper age limit of Late Cambrian for the Meson Group.

Low greenschist-facies metaclastic rocks in the vicinity of Tucumán (~26° to 27°S), upper greenschist to lower amphibolite-facies metaclastic rocks of the Ancasti Formation (~28° to 30°S Figure 1; Willner, 1983), and greenschist to upper amphibolite- and granulite-facies metaclastic rocks in Sierras de Córdoba (~31°S to 33°S, Figure 1), all included in the morphostructural province of Sierras Pampeanas (Ramos, 1999), have been considered as deep structural levels of the Puncoviscana Fm. (Willner and Miller, 1985; Toselli, 1990; Willner, 1990; Rapela *et al.*, 1998; Steenken *et al.*, 2004; Siegesmund *et al.*, 2010; Steenken *et al.*, 2011). Late Neoproterozoic (570–680 Ma) and Mesoproterozoic (960–1020 Ma) detrital zircon age maxima have been obtained from banded schists of the Ancasti Formation (U-Pb; Rapela *et al.*, 2007). Similarly, Neoproterozoic (600–700 Ma) and Mesoproterozoic (900–1000 Ma) detrital zircon age maxima characterize metasedimentary rocks from the Sierras de Córdoba (Rapela *et al.*, 1998; Schwartz and Gromet, 2004; Escayola *et al.*, 2007; Drobe *et al.*, 2009).

Sr and Nd-isotope data from Puncoviscana Fm. and higher-grade related rocks are relatively homogeneous, suggesting that most NW Argentinian basement rocks shared similar sources (Becchio *et al.*, 1999; Lucassen *et al.*, 2000). Nd-model (T_{DM}) ages from the low-grade Puncoviscana Formation range from 1600 to 1800 Ma (Bock *et al.*, 2000; Drobe *et al.*, 2009), and from 1700 to 1800 Ma in Sierras de Córdoba metasedimentary rocks (Rapela *et al.*, 1998; Steenken *et al.*, 2011; Drobe *et al.*, 2011). Similar T_{DM} model ages (average T_{DM} age $\sim 1.76 \pm 0.4$ Ga) were reported from Sierra de Quilmes metasedimentary rocks (Figure 1; Lucassen *et al.*, 2000).

In Sierras de Córdoba, a main migmatization event occurred at ~530 Ma (U/Pb SHRIMP zircon ages; Rapela *et al.*, 1998, 2002). Although its significance is still not very well constrained and further geochronological work may be necessary, an earlier 543 ± 3.6 Ma (U/Pb zircon age) metamorphic event has been proposed by Siegesmund *et al.* (2010) for high-grade non-migmatitic gneisses of Sierras de Córdoba (Sierra Grande). Similarly, a first Pampean metamorphic event has been dated as 540–570 Ma (Rb/Sr whole rock data; Bachmann and Grauert, 1986; Bachmann *et al.*, 1987) in banded schists of the Ancasti Formation.

The 523.7 ± 0.8 Ma calc-alkaline Cañaní pluton (U-Pb TIMS zircon age, Escayola *et al.*, 2011), and the 536 ± 7 Ma or 534 ± 7 Ma Santa Rosa de Tástil calc-alkaline granite (Figure 1a; U-Pb zircon ages of Bachmann *et al.*, 1987, and U-Pb Laser ICPMS zircon ages of Hauser *et al.*, 2011, respectively) were emplaced in the chevron-folded Puncoviscana Fm. and are interpreted as part of a 'Pampean' magmatic arc (Omarini *et al.*, 1999). In Sierras de Córdoba, the 530 ± 3 Ma calc-alkaline Sierra del Norte batholith (U-Pb zircon ages, Rapela *et al.*, 1998) is considered to be the southward extension of the Pampean magmatic arc (Lira *et al.*, 1997). Based on U-Pb zircon ages, Schwartz *et al.* (2008) suggested that the activity of this arc extended from *ca.* 555 to 525 Ma. The 522 ± 8 Ma (U-Pb monazite ages, Rapela *et al.*, 1998) and 515–520 Ma (U-Pb monazite ages, Gromet and Simpson, 1999, 2000) peraluminous granites and migmatites in Sierras de Córdoba contain xenoliths of folded metasediments, suggesting that shortening of these rocks occurred prior to migmatization (Piñán-Llamas and Simpson, 2006). K/Ar and Ar/Ar muscovite ages starting at 502 Ma (Krol and Simpson, 1999; Steenken *et al.*, 2010) and 505.7 ± 7.3 Ma ages (PbSL titanite age; Siegesmund *et al.*, 2010) likely indicate the end of the Pampean metamorphism in the Córdoba region (Siegesmund *et al.*, 2010; Steenken *et al.*, 2011).

A number of collisional and non-collisional models have been proposed to explain the Pampean orogeny. In non-collisional models, the Puncoviscana turbiditic sediments were initially passive margin deposits (*e.g.* Durand, 1996) that likely evolved into an accretionary prism due to eastward subduction in the lower Cambrian (Rapela *et al.*, 1998; Omarini *et al.*, 1999; Piñán-Llamas and Simpson, 2006). During this process, the Puncoviscana Fm. and higher-grade metasediments of the Sierras de Córdoba were intruded by the calc-alkaline 'Pampean' magmatic arc (or 'Tilcaric arc', Omarini *et al.*, 1999) and the Sierra del Norte complex (Figure 1a; Lira *et al.*, 1997; Schwartz *et al.*, 2008), respectively. The Pampean cycle ended with an episode of peraluminous magmatism, related to subduction of a mid-ocean ridge under the Puncoviscana accretionary prism as the arc magmatism was coming to a close (Fantini *et al.*, 1998; Simpson *et al.*, 2003; Schwartz *et al.*, 2008). Schwartz *et al.* (2008) suggest that east-dipping subduction at *ca.* 555 Ma was likely followed by the ridge-trench collision at 525 Ma. In alternative models based on structural and geochronological data, the Puncoviscana sediments are foreland (Zimmermann, 2005; Ramos, 2008), fore-arc (*e.g.* Astini *et al.*, 1996; Pankhurst *et al.*, 1997), or back-arc basin deposits (Omarini *et al.*, 1999; Escayola *et al.*, 2007; Collo *et al.*, 2009) tectonized in the mid-Cambrian Pampean orogeny.

In collisional models, the Puncoviscana Fm. and higher-grade related rocks were part of independent terranes (*e.g.* the 'Pampia terrane' of Ramos *et al.*, 1986 and Ramos, 1988) that collided with the western Gondwana margin during the Pampean orogeny. In related models, the Pampean orogeny

has been associated with the accretion of the allochthonous or para-autochthonous Pampia block (Rapela *et al.*, 1998; Ramos, 2008; Collo *et al.*, 2009) or the Western Sierras Pampeanas (Rapela *et al.*, 2007; Siegesmund *et al.*, 2009 and references therein) to the western margin of Gondwana. Consistent with collisional models is the presence of a discontinuous string of thin bodies of MORB-basalts in the Sierras de Córdoba that has been interpreted as a disrupted ophiolitic sequence (Escayola *et al.*, 2007; Ramos *et al.*, 2000; Rapela *et al.*, 1998; Steenken *et al.*, 2011).

Isotopic and geochronological affinities between the Puncoviscana Fm. and related metaclastic rocks to the south, and Gondwanan sources in South Africa, led some authors to propose an alternative model in which the Puncoviscana sediments were deposited in a trough marginal to the Kalahari craton and later emplaced against the western margin of the Rio de la Plata craton through a lateral strike-slip displacement (Rapela *et al.*, 2007; Casquet *et al.*, 2008; Drobe *et al.*, 2009, 2011; Siegesmund *et al.*, 2010). Based on Sm-Nd isotopic data and zircon provenance patterns, Collo *et al.* (2009) proposed that the Puncoviscana Fm. and equivalent protoliths within Sierras Pampeanas were deposited in a back-arc basin to the west of a Brasiliano magmatic arc that developed on a Mesoproterozoic basement extension of the Arequipa-Antofalla massif (Collo *et al.*, 2009).

After the Pampean orogeny, the Pacific margin of Gondwana turned into a passive margin. Magmatism and tectonism were resumed in the Early Ordovician during the Famatinian Orogeny (Aceñolaza and Toselli, 1973). Ordovician magmatism, dated as ~ 470 Ma (Büttner *et al.*, 2005; Dahlquist *et al.*, 2012) locally affected the Puncoviscana Fm., and high-grade equivalents, resetting isotopic systems (*e.g.* Sierra de Ancasti, Sierra de Quilmes). According to several models, the Arequipa, Cuyania/Precordillera, and Chilenia terranes were likely accreted to the Pacific margin of Gondwana (Ramos *et al.*, 1986; Ramos, 1988; Bahlburg and Hervé, 1997; Thomas and Astini, 2003; Collo *et al.*, 2009; Ramos, 2008, 2009; Steenken *et al.*, 2011; Drobe *et al.*, 2011) during the rest of the Paleozoic. Separation of the Pampean Orogen into isolated basement blocks with intervening pull-apart basins began in the late Carboniferous and continued through the Cretaceous. Exhumation of basement blocks on high-angle, Tertiary to Recent reverse faults has been related to the Andean orogeny (Jordan and Allmendinger, 1986).

3. Methodology

A total of 27 samples from the Puncoviscana Fm. (Cordillera Oriental) and higher-grade metaclastic sediments from Cumbres Calchaquies, Sierras de Ancasti, Quilmes, and Córdoba were collected for petrographic and geochemical analyses (approximate locations of the samples in Figure 1b; coordinates and description of the samples in

Appendix I). The analyzed samples include metapelites, massive psammities, and banded metapsammities that are the main lithologies present in the sampled areas. All samples were crushed. Fifty-five major, trace, and rare

earth elements were determined (Table 1) by Activation Laboratories Ltd. (Ontario, Canada) according to their Code 4Lithoresearch and Code 4B1 packages. These packages combine lithium metaborate/tetraborate fusion

Table 1. Whole-rock major, minor, and rare-earth element abundances for Puncoviscana Fm. and higher-grade related rocks. Upper continental crust values (UCC) from McLennan, 2001.

SAMPLE		PUNCO 1	Punco 2	56A	67A	55	54A	67B	PV2	63B	63	91	ANFAMA	84B2	94
SiO ₂	%	75.49	68.86	75.84	75.07	61.54	50.52	58.11	53.85	75.05	75.56	77.55	81.44	79.12	73.71
TiO ₂	%	0.54	0.68	0.61	0.85	0.82	1.08	0.79	0.94	0.72	0.53	0.49	0.43	0.43	0.58
Al ₂ O ₃	%	10.53	13.69	10.22	10.78	17.40	22.58	18.86	20.42	10.88	10.97	10.31	8.80	10.02	11.11
Fe ₂ O ₃ tot	%	3.35	4.84	3.41	4.87	6.94	8.49	8.18	8.68	3.89	2.64	2.77	2.67	3.39	3.96
MnO	%	0.04	0.05	0.12	0.06	0.06	0.10	0.11	0.09	0.07	0.04	0.07	0.05	0.05	0.07
MgO	%	1.08	1.37	0.66	1.58	2.91	3.69	3.4	3.65	1.56	1.19	1.09	1.05	1.48	2.12
CaO	%	1.73	0.82	1.57	0.47	0.28	0.34	0.26	0.27	1.69	1.64	2.26	1.25	0.95	1.36
Na ₂ O	%	2.49	2.85	2.67	2.29	2.08	1.41	1.1	2.02	2.95	2.82	2.15	2.5	1.83	3.1
K ₂ O	%	2.21	3.17	2.08	2	4.44	6.91	5.19	5.55	1.85	2.12	2.08	1.44	2.13	1.37
P ₂ O ₅	%	0.18	0.21	0.2	0.21	0.17	0.21	0.16	0.2	0.21	0.2	0.18	0.16	0.12	0.18
LOI	%	2.83	2.74	2.41	2.07	3.58	4.84	4.27	4.1	0.58	2.48	1	0.47	0.88	2.39
Total	%	100.47	99.28	99.79	100.25	100.22	100.18	100.43	99.77	99.44	100.19	99.94	100.26	100.40	99.95
CIA		53.34	60.03	53.10	63.15	67.59	69.45	71.46	68.57	53.57	53.74	52.11	53.77	59.71	56.28
ICV		1.08	1.00	1.08	1.12	1.00	0.97	1.00	1.03	1.16	1.00	1.05	1.06	1.02	1.12
Ba	ppm	178	247	320	232	340	479	575	624	357	296	287	205	229	210
Rb	ppm	99	131	95	89	198	282	226	230	79	86	102	66	90	64
Sr	ppm	67	55	62	51	44	36	24	46	188	103	212	111	120	103
V	ppm	58	82	61	89	113	164	130	154	68	54	49	39	48	62
Cr	ppm	40	60	40	60	90	120	100	120	60	50	40	40	40	50
Ni	ppm	20	30	< 20	< 20	30	40	40	40	< 20	< 20	< 20	< 20	20	30
Co	ppm	8	13	8	10	20	23	23	26	9	8	7	6	9	14
Cu	ppm	< 10	< 10	20	10	30	30	30	100	< 10	< 10	10	10	10	20
Y	ppm	27.6	25.3	33.8	32	36.8	44.9	27.7	39	29.7	24.9	25.8	18.8	22.8	26.3
Zr	ppm	365	173	581	534	178	223	147	176	330	236	247	243	138	179
Cs	ppm	3.8	7	5.3	4.2	12.7	18.3	10.3	13.2	5.2	5.2	5.5	4.1	4.4	3.3
Hf	ppm	9.9	4.6	15.2	13.5	4.7	6.2	4.2	4.9	8.5	6.3	6.8	6.3	3.7	4.8
Nb	ppm	9.8	11.3	10.9	13	16.4	20.2	14.3	18	10.7	9.6	9.7	7.6	5.7	7.8
Ta	ppm	1.04	1.17	1.06	1.22	1.49	1.9	1.42	1.61	1.05	0.93	0.95	0.71	0.6	0.75
Pb	ppm	12	22	13	17	9	16	22	6	17	7	19	10	7	13
Sc	ppm	8	11	8	10	17	23	19	22	9	8	7	6	6	9
Zn	ppm	60	100	80	70	130	140	150	170	50	60	60	50	70	180
Th	ppm	10.3	11.4	11	12.1	15.6	20.3	15.8	19.1	11.6	8.99	8.64	7.25	5.24	6.92
U	ppm	2.64	2.44	3.01	2.87	3.63	4.87	3.25	6.93	2.55	2.03	1.89	1.7	1.57	1.93
La	ppm	34.3	32.8	40.8	47.8	45.6	38.7	25.3	39.6	32.2	32	29	23.1	20.1	27.3
Ce	ppm	70.2	64.2	83.4	96.5	94.1	81.7	52.1	84.7	67.9	63.4	56.3	52.8	43.3	57.9
Pr	ppm	7.99	7.41	9.41	10.8	9.96	8.74	5.86	9.39	8.08	7.14	6.84	5.43	5.17	6.69
Nd	ppm	29.9	27.3	35.2	40.9	38.4	33.7	21.8	36	31.4	27.7	25.4	21.2	20.8	26.5
Sm	ppm	5.86	5.46	6.81	7.83	7.46	7.2	4.41	6.79	6.36	5.19	4.98	4.03	4.37	5.25
Eu	ppm	1.17	1.08	1.28	1.47	1.43	1.56	0.996	1.12	1.31	1.13	1.08	0.874	1.12	1.15
Gd	ppm	5.42	4.95	6.22	6.79	6.93	7.3	4.38	5.83	5.71	4.86	4.59	3.6	4.33	4.86
Tb	ppm	0.88	0.84	1.02	1.1	1.13	1.4	0.83	0.95	0.95	0.75	0.76	0.57	0.75	0.8
Dy	ppm	5.09	4.81	5.85	5.91	6.43	8.25	5.01	5.58	5.33	4.35	4.3	3.33	4.12	4.59
Ho	ppm	0.98	0.92	1.12	1.1	1.23	1.59	0.99	1.24	1.04	0.82	0.83	0.65	0.8	0.89
Er	ppm	2.97	2.74	3.37	3.31	3.61	4.79	3.02	4.03	3.18	2.46	2.45	1.97	2.32	2.64
Tm	ppm	0.446	0.446	0.519	0.514	0.546	0.73	0.486	0.654	0.501	0.385	0.381	0.319	0.335	0.386
Yb	ppm	2.94	2.81	3.41	3.35	3.51	4.74	3.21	4.26	3.25	2.55	2.5	2.15	2.12	2.44
Lu	ppm	0.449	0.396	0.547	0.519	0.513	0.682	0.5	0.637	0.506	0.385	0.378	0.327	0.326	0.379
Li	ppm	2	3	2	2	3	5	3	4	2	2	2	1	1	2
ΣREE		168.60	156.16	198.96	227.89	220.85	201.08	128.89	200.78	167.72	153.12	139.79	120.35	109.96	141.78
Zr/Sc		45.63	15.73	72.63	53.40	10.47	9.70	7.74	8.00	36.67	29.50	35.29	40.50	23.00	19.89
Th/Sc		1.29	1.04	1.38	1.21	0.92	0.88	0.83	0.87	1.29	1.12	1.23	1.21	0.87	0.77
Nb/Y		0.36	0.45	0.32	0.41	0.45	0.45	0.52	0.46	0.36	0.39	0.38	0.40	0.25	0.30
La/Sc		4.29	2.98	5.10	4.78	2.68	1.68	1.33	1.80	3.58	4.00	4.14	3.85	3.35	3.03
La/Th		3.33	2.88	3.71	3.95	2.92	1.91	1.60	2.07	2.78	3.56	3.36	3.19	3.84	3.95
Th/U		3.90	4.67	3.65	4.22	4.30	4.17	4.86	2.76	4.55	4.43	4.57	4.26	3.34	3.59
Cr/V		0.69	0.73	0.66	0.67	0.80	0.73	0.77	0.78	0.88	0.93	0.82	1.03	0.83	0.81
Cr/Th		3.88	5.26	3.64	4.96	5.77	5.91	6.33	6.28	5.17	5.56	4.63	5.52	7.63	7.23
Eu/Eu*		0.63	0.63	0.60	0.62	0.61	0.66	0.69	0.54	0.66	0.69	0.69	0.70	0.79	0.70
Ce/Ce*		0.99	0.96	1.00	1.00	1.03	1.04	1.00	1.03	0.99	0.98	0.94	1.10	1.00	1.00
(La/Yb) _n		7.88	7.89	8.09	9.64	8.78	5.52	5.33	6.28	6.70	8.48	7.84	7.26	6.41	7.56
(La/Sm) _n		3.68	3.78	3.77	3.84	3.85	3.38	3.61	3.67	3.19	3.88	3.67	3.61	2.90	3.27
(Gd/Yb) _n		1.49	1.43	1.48	1.64	1.60	1.25	1.11	1.11	1.42	1.54	1.49	1.36	1.66	1.61

Table 1. (Continuation).

SAMPLE		77	84B1	63AC	9306-2	9307-2	9306-1	9307-1	9846-2	9677-2	9847.000	9846-1	9677-1	9848-1	UCC
SiO ₂	%	77.14	64.28	78.30	77.17	76.02	58.94	54.09	77.08	73.44	68.28	57.36	47.78	52.26	66.00
TiO ₂	%	0.68	0.77	0.59	0.48	0.52	0.96	1.14	0.48	0.54	0.90	0.94	1.30	1.10	0.50
Al ₂ O ₃	%	10.45	17.99	9.91	10.92	11.37	19.09	21.29	10.82	11.58	15.24	20.84	22.31	22.66	15.20
Fe ₂ O ₃ tot	%	3.98	5.20	3.51	3.72	4.24	6.87	7.68	3.65	4.20	6.37	6.26	10.94	8.49	4.50
MnO	%	0.05	0.08	0.08	0.05	0.06	0.08	0.12	0.06	0.06	0.12	0.10	0.15	0.11	0.08
MgO	%	1.82	2.21	1.45	1.78	1.74	3.29	3.05	1.62	1.84	2.53	2.73	4.81	4.24	2.20
CaO	%	0.38	0.9	1.64	0.87	0.33	1.34	0.55	0.92	1.24	1.00	1.51	1.95	1.53	4.20
Na ₂ O	%	2.85	1.77	2.37	1.51	2.15	2.38	2.68	1.76	2.17	1.20	2.78	3.45	1.92	3.90
K ₂ O	%	1.38	4.85	1.62	2.25	2.41	4.56	5.61	2.46	2.32	3.88	4.96	5.29	5.15	3.40
P ₂ O ₅	%	0.2	0.16	0.18	0.13	0.17	0.15	0.26	0.13	0.22	0.14	0.20	0.29	0.29	0.17
LOI	%	1.65	1.98	0.64	1.47	1.55	2.51	2.89	0.89	0.88		2.11	1.56	2.67	
Total	%	100.58	100.18	100.29	100.35	100.56	100.16	99.36	99.86	98.49	99.65	99.80	99.83	100.42	100.15
CIA		62.02	65.61	54.69	63.80	64.18	63.57	66.19	60.97	59.70	66.52	63.03	60.99	67.65	
ICV		1.06	0.87	1.13	0.97	1.00	1.02	0.97	1.01	1.06	0.98	0.92	1.24	0.99	
Ba	ppm	258	662	243	297	261	570	615	289	303	615.68	694	551	779	550
Rb	ppm	58	160	73	95	96	205	222	93	96	132.46	174	242	225	112
Sr	ppm	73	116	130	98	53	162	96	114	116	81.28	187	201	120	350
V	ppm	61	100	59	82	63	151	141	53	74		119	156	151	107
Cr	ppm	50	80	50	50	50	110	120	40	50	81.78	90	160	140	83
Ni	ppm	< 20	20	< 20	< 20	< 20	40	40	< 20	30		30	60	50	44
Co	ppm	11	15	8	12	11	25	21	10	12	23.11	17	32	24	17
Cu	ppm	20	10	10	20	20	20	20	< 10	10	6.47	< 10	30	30	25
Y	ppm	32.4	40.5	31.5	22	26.6	37.3	41.7	24.2	22.2	28.50	44	48.1	48.7	22
Zr	ppm	317	255	283	132	157	169	262	149	144	132.26	269	201	225	190
Cs	ppm	3.6	7.5	5.7	6.9	5.9	13.5	11.4	5.3	6.2	7.26	8.3	16.8	12.4	4.6
Hf	ppm	8.2	6.7	7.7	3.6	4.4	4.5	7.3	4	3.8	3.83	7.1	6	6.6	5.8
Nb	ppm	10.4	13.8	7.9	7.5	10.3	14.9	19.9	6.6	7.5	13.04	12.7	18.3	18.1	12
Ta	ppm	1	4.08	0.77	0.73	1.03	1.32	1.92	0.6	0.74	0.86	1.18	1.93	1.75	1
Pb	ppm	8	9	54	21	12	32	17	6	23	30.00	10	40	28	17
Sc	ppm	8	14	8	9	9	17	20	7	10	15.76	16	25	21	13.6
Zn	ppm	60	110	140	90	90	160	150	50	80	129.09	100	180	190	71
Th	ppm	10.2	10.2	8.6	6.22	9.02	11.7	21.4	6.03	6.86	6.95	12.1	19.2	16.2	10.7
U	ppm	2.53	2.98	2.4	1.53	1.92	2.7	3.06	1.82	2.22	2.12	3.61	4.85	4	2.8
La	ppm	35.8	35.5	31	21.3	38.3	35.2	47.2	21.2	24	24.60	42	63.3	52.3	30
Ce	ppm	69.7	75.4	66.5	44.9	79.1	72.4	96.9	46.2	51	51.16	88	130	106	64
Pr	ppm	8.74	8.75	7.74	5.15	8.63	8.23	11.2	5.28	5.91	6.25	10.3	14.3	12.3	7.1
Nd	ppm	35.6	35.1	30.7	21	32.7	32.8	42.3	21.6	23.6	25.50	41.4	56.9	47.1	26
Sm	ppm	7.07	7.56	6.33	4.42	6.23	6.78	8.96	4.53	5.01	5.56	8.79	10.6	9.38	4.5
Eu	ppm	1.46	1.63	1.33	1.03	1.23	1.54	1.68	1.15	1.13	1.03	1.92	2.6	1.91	0.88
Gd	ppm	6.78	7.15	6.17	4.12	5.63	6.76	8.18	4.41	4.94	5.13	8.52	10	8.69	3.8
Tb	ppm	1.05	1.21	1	0.67	0.91	1.12	1.39	0.74	0.78	0.76	1.42	1.58	1.47	0.64
Dy	ppm	5.92	6.89	5.79	3.82	4.92	6.45	7.79	4.38	4.37	4.93	7.94	9.22	8.2	3.5
Ho	ppm	1.11	1.34	1.09	0.74	0.9	1.2	1.48	0.84	0.82	0.97	1.49	1.77	1.55	0.8
Er	ppm	3.28	4.02	3.17	2.16	2.68	3.45	4.39	2.53	2.36	2.91	4.41	5.23	4.57	2.3
Tm	ppm	0.493	0.586	0.47	0.32	0.41	0.52	0.66	0.38	0.35	0.41	0.68	0.79	0.70	0.33
Yb	ppm	3.2	3.72	3.07	2.08	2.6	3.4	4.2	2.46	2.26	2.73	4.38	5.02	4.44	2.2
Lu	ppm	0.475	0.568	0.463	0.325	0.378	0.518	0.658	0.373	0.327	0.40	0.631	0.769	0.663	0.32
Li	ppm	2	1	2	2	2	4	4	1	< 1		2	2	6	
ΣREE		180.68	189.42	164.83	112.04	184.62	180.37	236.99	116.07	126.86	132.34	221.88	312.08	259.27	146.37
Zr/Sc		39.63	18.21	35.38	14.67	17.44	9.94	13.10	21.29	14.40	8.39	16.81	8.04	10.71	13.97
Th/Sc		1.28	0.73	1.08	0.69	1.00	0.69	1.07	0.86	0.69	0.44	0.76	0.77	0.77	0.79
Nb/Y		0.32	0.34	0.25	0.34	0.39	0.40	0.48	0.27	0.34	0.46	0.29	0.38	0.37	0.55
La/Sc		4.48	2.54	3.88	2.37	4.26	2.07	2.36	3.03	2.40	1.56	2.63	2.53	2.49	2.21
La/Th		3.51	3.48	3.60	3.42	4.25	3.01	2.21	3.52	3.50	3.54	3.47	3.30	3.23	2.80
Th/U		4.03	3.42	3.58	4.07	4.70	4.33	6.99	3.31	3.09	3.28	3.35	3.96	4.05	3.82
Cr/V		0.82	0.80	0.85	0.61	0.79	0.73	0.85	0.75	0.68		0.76	1.03	0.93	0.78
Cr/Th		4.90	7.84	5.81	8.04	5.54	9.40	5.61	6.63	7.29	11.76	7.44	8.33	8.64	7.76
Eu/Eu*		0.64	0.68	0.65	0.74	0.63	0.70	0.60	0.79	0.69	0.59	0.68	0.77	0.65	0.65
Ce/Ce*		0.92	1.00	1.01	1.00	1.02	1.00	0.99	1.02	1.00	0.97	0.99	1.01	0.98	1.07
(La/Yb) _n		7.56	6.45	6.82	6.92	9.95	7.00	7.59	5.82	7.18	6.10	6.48	8.52	7.96	9.21
(La/Sm) _n		3.19	2.96	3.08	3.03	3.87	3.27	3.32	2.95	3.02	2.79	3.01	3.76	3.51	4.20
(Gd/Yb) _n		1.72	1.56	1.63	1.61	1.75	1.61	1.58	1.45	1.77	1.53	1.58	1.61	1.59	1.40

ICP analysis for major elements with ICP-MS analysis for trace elements, using international rock standards (Activation Laboratories Ltd. 2006). According to replicates and standard results, the analytical precision was typically

better than $\pm 2.3\%$ for most major elements and better than $\pm 10\%$ for trace elements. In the discussion we also include previously published compositions of metaclastic rocks from Sierra de Ancasti, and the Puncoviscana Fm. (data

from Do Campo and Ribeiro-Guevara, 2005; Willner *et al.*, 1985; and Zimmermann, 2005). In the following sections we summarize lithological, structural, petrographic, and microstructural observations from the analyzed samples and their outcrops.

4. Sample Description

4.1. Puncoviscana Formation-Anchizone grade

The Puncoviscana Fm. consists of anchizone-grade centimeter- to meter-thick massive metapsammitic beds alternating with centimeter-thick green and red metapelitic layers, and centimeter- to meter-thick layers of banded metapsammites. Massive metapsammitic layers containing graded- and cross-bedding and parallel lamination gradually transition into metapelitic layers. Three massive metapsammites (Punco 1, Punco 2, 56A), a banded metapsammitic (67A), and four metapelitic samples (55, 54A, 67B, PV2) were collected for analysis (locations in Appendix I). In thin section, massive metapsammites and quartz-rich bands in banded metapsammitic samples are characterized by subangular, poorly sorted clasts of quartz, feldspar (mostly albite and minor K-feldspar), and rock fragments (quartzite, siltstone, shales, phyllites), clays, small detrital white micas, and few chlorite grains. Zircon, rutile, magnetite, and tourmaline are also present. In metapelitic rocks, elongated quartz grains with curved grain boundaries and pressure shadows are present. A compaction-related, bedding-parallel cleavage (S_c) is defined by aligned detrital micas, pressure-solution seams, and micabeards in banded and massive metapsammites, and metapelitic samples. Although Tertiary (Andean) deformation locally overprints older tectonic structures, predominant Pampean structures consist of N-S metric to decimetric chevron folds with mostly subhorizontal axes (Figure 1b) and subvertical axial planes that fold bedding and S_c . An S_1 fanning cleavage associated with chevron folds intersects bedding and S_c , and is observed mostly in metapelitic rocks (Piñán-Llamas and Simpson, 2006, 2009).

4.2. Metaclastic rocks from Cumbres Calchaquies (26°S - 27°S)- Low-Greenschist facies

Low greenschist-facies metaclastic sequences in northern Cumbres Calchaquies (Fm Medina, Gonzalez *et al.*, 2000) include centimeter- to meter-thick levels of banded metapsammites, centimeter- to meter-thick massive metapsammitic beds, and centimeter-thick metapelitic beds. Cross- and graded-bedding, parallel lamination, slumps, and flame structures are preserved in metapsammites. Seven banded metapsammitic samples (63B, 63, 91, Anfama, 84B2, 94, 77) and one metapelitic sample (84B1) were analyzed for geochemistry (Figure 1b; Appendix I). Similarly to anchizone-grade samples, quartz-rich bands

in banded metapsammitic samples are petrographically characterized by subangular quartz, feldspar (mostly albite), and rock fragments (quartzite, siltstone, shales). Local matrix recrystallization is observed. In both massive and banded metapsammitic samples, fine-grained detrital micas are preserved, but metamorphic white mica (illite; Toselli and Rossi de Toselli, 1983a, 1983b) and chlorite grains are more abundant than in lower-grade samples. Zircon, apatite, rutile, ilmenite, and tourmaline are common accessory minerals in metapsammitic samples. In thin section, a bedding-parallel cleavage (S_c) is defined in metapelitic and metapsammitic samples by preferentially oriented detrital and metamorphic white micas and chlorite, elongated quartz grains with partially dissolved borders, and pressure-solution seams. A tectonic cleavage (S_1) associated with NNE-SSW metric to decimetric chevron folds is present in metapelitic and metapsammitic rocks. These folds, are characterized by subhorizontal axes (Figure 1b) and subvertical axial planes. In thin section, S_1 is defined by asymmetric quartz grains with dissolved borders and pressure shadows, pressure-solution seams, preferentially aligned metamorphic white micas, and chlorite grains. At outcrop scale, S_1 is observed as a fanning cleavage overprinting bedding and S_c (Piñán-Llamas and Simpson, 2006, 2009).

4.3. NE Sierra de Quilmes

In northeastern Sierra de Quilmes, the Tolombon Complex (Toselli *et al.*, 1978) includes centimeter- to meter-thick banded metapsammitic levels, and centimeter-scale metapelitic layers. Relict bedding surfaces and cross bedding are preserved. Banded metapsammites are defined by 2-10 mm-thick quartz-rich domains alternating with 0.25-2.5 mm-thick biotite-rich domains. This compositional banding is subparallel to relict bedding. A quartz-rich banded metapsammitic sample (63AC) was collected for geochemical analysis (Figure 1b). In thin section, banded metapsammites are characterized by quartz-rich domains of recrystallized quartz with few interspersed plagioclase and biotite grains; biotite-rich bands are predominantly formed by large corroded and kinked biotite grains with quartz and opaque inclusions. Zircon, apatite, ilmenite, and tourmaline are accessory minerals in these rocks. Relict bedding and compositional banding are folded by NNE-SSW trending metric to decametric-scale chevron folds (Figure 1b) and cm-scale parasitic folds (F_1) with subvertical axial planes and subhorizontal axis. Cleavage associated with these folds (S_1) crosscuts the relict bedding and compositional banding. S_1 is defined by preferentially aligned large idiomorphic metamorphic biotite grains and, locally, by small white micas.

4.4. Ancasti Formation

The Ancasti Formation (Figure 1) includes metric to cm-thick metapelitic levels with interlayered psammitic lenses,

massive metapsammitic levels, and banded metapsammites (Willner and Miller, 1982; Willner, 1983). The compositional banding is subparallel to bedding relicts. Two samples of banded metapsammites (9306-2, 9307-2) and two samples of metapelites (9306-1, 9307-1) were geochemically analyzed (location and description of the samples in Appendix I). Banded metapsammites are characterized by alternating thin biotite-rich and thicker granoblastic quartz-rich layers that include small interspersed biotite grains and plagioclase (mostly albite). NNW to N-S trending upright cm-scale F_1 folds with an associated axial plane cleavage (S_1) affect bedding relicts and compositional banding. Preferentially oriented idiomorphic biotite grains define S_1 .

4.5. Tuclame Formation

Centimeter- to meter-thick layers of metapelites and meter- to several meters-thick banded metapsammites occur along the westernmost edge of the Sierras de Córdoba (the Tuclame Formation, Figure 1). Banded metapsammites are characterized by a monotonous compositional banding, which is subparallel to bedding relicts, defined by cm-thick quartz-rich bands alternating with 2–5-mm thick biotite-rich layers. A very similar compositional banding occurs in lower-grade rocks of the Puncoviscana Fm., where primary structures are well preserved. Three samples of banded psammites (9846-2, 9677-2, 9847) and three metapelitic samples (9846-1, 9677-1, 9848-1) were geochemically analyzed (Figure 1b). In thin section, banded schists are characterized by granoblastic quartz-rich bands, that include sub-equant to elongate quartz grains, interspersed albite, and tabular biotite grains; occasionally, detrital quartz and feldspar grains are preserved. These quartz-rich bands alternate with biotite-rich bands defined by deformed biotite grains with quartz, feldspar, and muscovite inclusions. Centimeter- to decimeter-scale F_1 folds with N-S to NNW-SSE trending axes (Figure 1b) and subvertical axial planes affect the compositional banding and bedding relicts. Euhedral metamorphic biotites associated with F_1 folds define an axial planar disjunctive cleavage (S_1) that crosscuts the compositional banding.

5. Results

Geochemistry can be used to constrain the provenance and tectonic setting of sedimentary and metasedimentary rocks if their original whole-rock composition was not significantly altered during diagenesis, weathering, and/or metamorphism, (McLennan *et al.*, 1993). In metamorphic rocks, immobile trace elements and REE are particularly reliable in the study of their provenance and depositional setting (McLennan, 1989; McLennan *et al.*, 1990; 1993; Girty *et al.*, 1994).

5.1. Weathering and sorting

The degree of weathering can be quantitatively measured with the Chemical Index of Alteration (Nesbitt and Young, 1982), defined as $Al_2O_3/[Al_2O_3 + CaO^* + Na_2O + K_2O] \times 100$ (molar contents, with CaO^* being CaO content in the silicate fraction of the sample). The CIA measures the extent to which feldspars have been transformed into aluminous clays depleted in Ca, Na, and K relative to the unweathered source. On a scale of 40–100, unweathered igneous rocks have CIA values of 45–55, while values for moderately weathered shales range from 70 to 75 CIA. Intense weathering of feldspars in a rock results in high concentrations of residual clays (kaolinite and/or gibbsite), producing CIA values close to 100. CIA values for our samples (Table 1) vary between ~52 and 72, with an average value of 57 ($n = 20$) for metapsammites, and a mean of 67 for metapelitic samples ($n = 11$), thus showing a moderate degree of weathering. High-silica concentration in metapsammitic samples could mask the alteration, resulting in low CIA values (Nesbitt and Young, 1982).

Our data and previously published geochemical data for metapelitic and metapsammitic samples from the Puncoviscana and Ancasti formations (Zimmermann, 2005; Willner *et al.*, 1985; Do Campo and Ribeiro-Guevara, 2005) are plotted on a ternary diagram using molecular proportions of $Al_2O_3 - (CaO^* + Na_2O) - K_2O$ (A–CN–K diagram; Figure 2a and 2b) to evaluate deviation of the composition of the metasedimentary rocks from their original source (Nesbitt and Young, 1984; 1989). In this plot, an ideal trend almost parallel to the $Al_2O_3 - (CaO^* + Na_2O)$ axis from a fresh unweathered homogeneous source indicates no significant change in the metasedimentary rocks ($CaO^* + Na_2O$) and K_2O ratio with respect to the source. Our samples define a general trend toward illite-muscovite compositions (Figure 2a). K-feldspar is generally scarce in Puncoviscana Fm. metaclastic rocks (Do Campo and Ribeiro-Guevara, 2005; Zimmermann, 2005), and the composition of plagioclase is mostly albitic (Do Campo and Nieto, 2003). Therefore, the relatively high K content in the samples may be related to the transformation of aluminous clay minerals to illite (Fedo *et al.*, 1995) or to secondary loss of Ca with respect to the parental material in the silicate fraction. Additionally, in an A–CN–K triangular plot, the intersection of the weathering trend with the feldspar join can be used to constrain initial compositions of source rocks (Fedo *et al.*, 1995). The intersection of the weathering trend defined by our samples with the feldspar join suggests a source rock with a plagioclase/K-feldspar ratio of approximately 4:2 (Figure 2a). This indicates that, according to the present A–CN–K values, our sample set may have been derived from weathering of granodioritic and/or granitic sources. This interpretation has to be considered with caution, since some mobilization of alkalis may have occurred.

The index of compositional variability (ICV = $[Fe_2O_3 + K_2O + Na_2O + CaO + MgO + TiO_2]/Al_2O_3$) measures the maturity of a sample based on the abundance

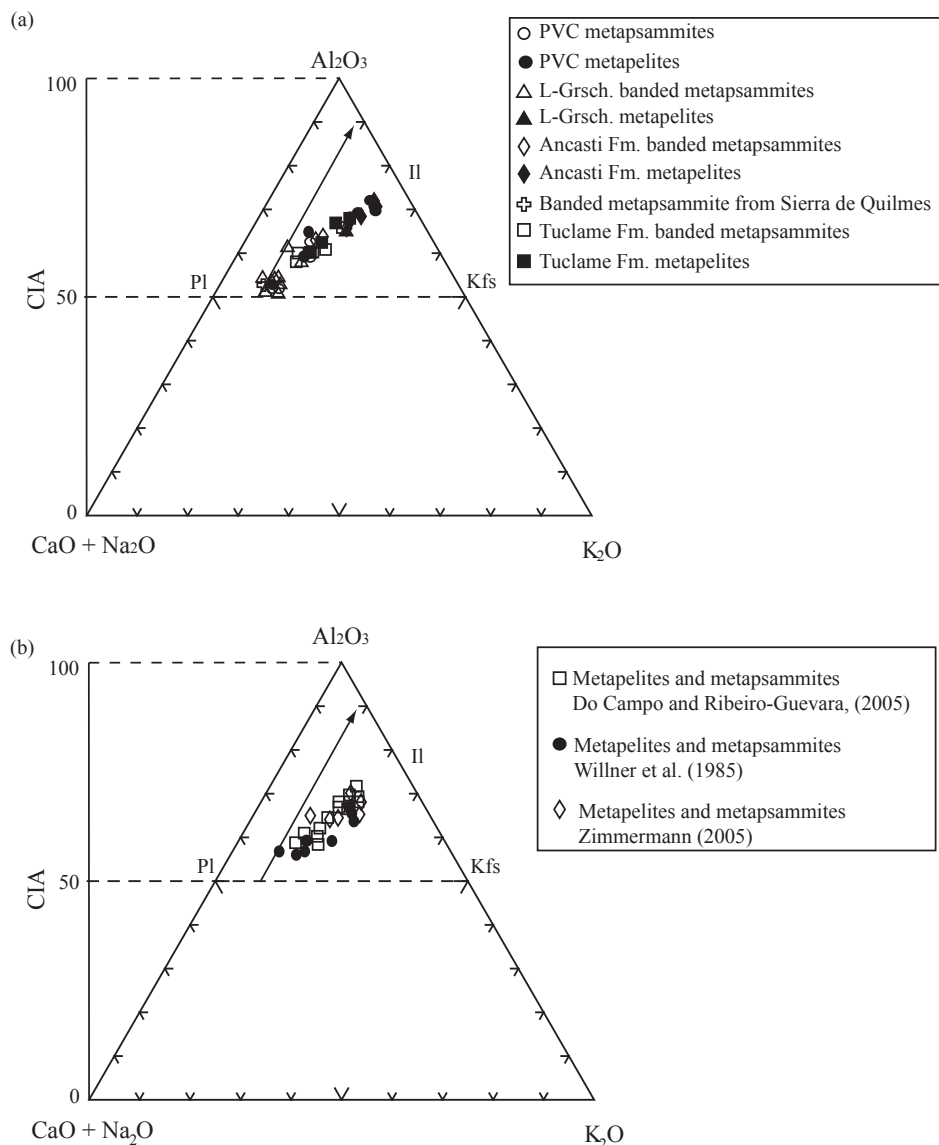


Figure 2. A-CN-K and CIA plot (after Fedo *et al.*, 1995) for the Puncoviscana Fm. and higher-grade related rocks showing their weathering trend. Arrow is an ideal weathering trend for upper continental crust. PVC, Anchizone-grade Puncoviscana Fm.; L-Grsch., Low-greenschist facies metaclastic rocks; Il, illite; Kfs, alkali feldspar; Pl, plagioclase; CIA after Nesbitt and Young (1982). (a) Samples investigated in this study. (b) Metapsammitic and metapelitic samples of the Puncoviscana Fm. from Zimmermann (2005), and Do Campo and Ribeiro-Guevara (2005). Also included are data for metapsammitic and metapelitic samples from the Ancasti Fm. from Willner *et al.* (1985).

of alumina relative to other major cations (Cox *et al.*, 1995). Non-clay minerals have higher ICV values than clay minerals and therefore, ICV values will decrease with increasing degree of weathering and/or maturity in the sample. Our samples display an average ICV = 1.03 (range = 0.87 - 1.24), suggesting moderate weathering and/or maturity of the source.

Zr/Sc ratios, considered good indicators of sediment recycling, show significant variation in our samples (Table 1), ranging between 7.74 and 72.63. Seven samples of anchizone and greenschist-grade banded metapsammites show the highest zircon enrichment with Zr/Sc > 30 ratios (Table 1). Non-recycled sediments show a simple positive

correlation between Th/Sc and Zr/Sc, while recycled sediments show a more rapid increase in Zr/Sc than in Th/Sc due to zircon enrichment (McLennan *et al.*, 1993). The general Th/Sc vs. Zr/Sc trend defined by our metapsammitic samples and previously published data for the Puncoviscana Fm. (Zimmermann, 2005, and Do Campo and Ribeiro-Guevara, 2005) is consistent with zircon concentration (Figure 3). In an Al_2O_3 - TiO_2 -Zr plot (García *et al.*, 1994) low-grade metaclastic samples define a trend toward the Zr apex, suggesting zircon accumulation (Figure 4). High TiO_2 values (Table 1) point to concentration of rutile and ilmenite. Relatively high REE concentrations in our low-grade samples (Table 1) compared to UCC values (average

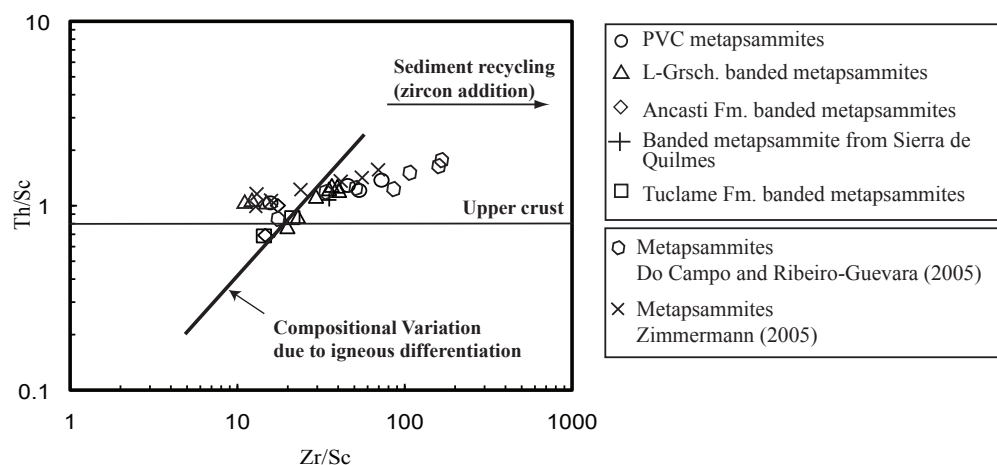


Figure 3. Th/Sc vs. Zr/Sc provenance and recycling discrimination plot (after McLennan *et al.*, 1990) for Puncoviscana Fm. and higher-grade related metapsammitic rocks. Th/Sc > 0.8 reflects provenance of samples from the upper continental crust (McLennan, 2001). High Zr/Sc ratios in low-grade psammitic samples suggest a higher degree of recycling. PVC, Anchizone-grade Puncoviscana Fm.; L-Grsch., Low-greenschist facies metaclastic rocks. Also included are data for metapsammitic samples of the Puncoviscana Fm. from Zimmermann (2005), and Do Campo and Ribeiro-Guevara (2005).

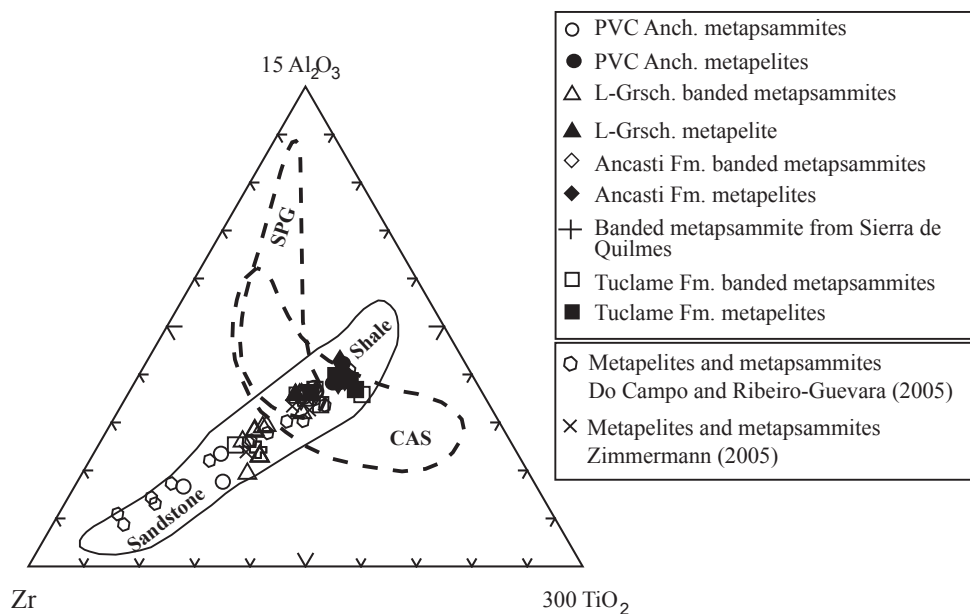


Figure 4. Al-Ti-Zr triangular diagram (after García *et al.*, 1994) for the Puncoviscana Fm. and higher-grade related rocks. PVC, Anchizone-grade Puncoviscana Fm.; L-Grsch., Low-greenschist facies metaclastic rocks. Solid contour encloses the compositions of the samples. CAS, Calc-alkaline suites; SPG, strongly peraluminous granites.

$\Sigma\text{REE} = 146$; McLennan, 1989) are also consistent with enrichment in heavy minerals.

High concentration of heavy minerals in sedimentary and metasedimentary rocks can be attributed to either, recycling of sediments or hydraulic sorting. In our samples, resistant heavy minerals include zircon, rutile, and ilmenite. V and Ti are mainly present in ilmenite and rutile. V and Ti show little correlation with Zr. Ilmenite is less resistant than zircon over multiple cycles of transport and weathering, and thus, the high concentration of zircon in some of the psammitic samples is likely due to recycling. Metapsammitic samples

display a relatively wide range of TiO_2 -Zr variations in an Al-Ti-Zr ternary diagram (Figure 4) thus supporting some reworking and recycling particularly in the low-grade rocks (García *et al.*, 1994).

5.2. Provenance

Our samples are characterized by a chemical composition similar to the upper continental crust (UCC, McLennan *et al.*, 1990; McLennan, 2001; Table 1). However, compared to UCC, metapelitic samples are more enriched in K, Rb,

U, V, Cs, Cr, Ti, Y, La, Ce, and Sc, and depleted in Sr, Nb, and Ta. Banded metapsammitic samples are characterized by enrichment in Cs, V, Cr, and depletion in Sr, Ba, Ta and Nb with respect to UCC. Few low-grade banded metapsammitic samples are enriched in Zr and Hf with respect to UCC.

Sc, Th, Zr, REE, and high field strength trace elements (HFSE) are reliable chemical elements in provenance analysis of sediments and metasedimentary rocks due to their insolubility and immobile character during transport, diagenesis, weathering, and metamorphism (McLennan and Taylor, 1991; McLennan *et al.*, 1995). Element ratios, such as Cr/V, La/Sc, Th/Co, Th/Sc, Cr/Th, and Eu/Eu*, are particularly useful in the study of the chemical composition of the source rocks (Taylor and McLennan, 1985; McLennan *et al.*, 1990; Cullers, 1994; Girty *et al.*, 1994). Additionally, incompatible and compatible element ratios are diagnostic in the identification of felsic and mafic source components (Cullers, 1994; Cox *et al.*, 1995; Fedo *et al.*, 1996).

The Th/Sc ratio is a reliable marker for source composition and the identification of mafic source components (McLennan *et al.*, 1990; McLennan and Taylor, 1991). Th is highly incompatible, and more abundant in crustal sources. Thus, the Th/Sc ratio will be high in rocks derived from the crust and low in rocks with a mantle origin. Our samples show Th/Sc ratios between 0.69 and 1.2 (average 0.95), consistent with upper crustal compositions (average Th/Sc ratio for UCC = 0.79, McLennan, 2001). Low-grade banded metapsammites generally display higher

Th/Sc ratios than banded metapsammites from Sierras de Ancasti and Córdoba (Table 1), likely indicating a higher sedimentary input from more evolved sources compared to higher-grade samples. Generally, high Rb/Sr ratios (74 % of our samples show Rb/Sr ratios > 0.80) and low Cr/V ratios (0.61-1.03) also point to non-mafic sources (McLennan *et al.*, 1993). Cr/Th ratios (average 6.28 ± 1.4) suggest felsic sources (Cullers, 1994). These ratios are generally lower in anchizone-grade (average Cr/Th = 4.70) and low-greenschist facies banded metapsammites (average Cr/Th = 5.81) than in higher-grade metapsammitic samples (Ancasti Fm. average Cr/Th = 6.47; Tuclame Fm. average Cr/Th = 8.56). Eu/Eu* values in our samples (average 0.67 ± 0.06) point to felsic sources (Cullers, 1994); K/Rb ratios (between 188 and 221) are close to those from typical differentiated magmatic suites (average ratio = 230; Shaw, 1968).

La/Th ratios are useful indicators of mafic or felsic source components, while Hf typically reveals the degree of recycling. On a La/Th vs. Hf plot (Floyd and Leveridge, 1987), a large group of metapsammitic samples show La/Th ratios and Hf contents that are compatible with evolved ("acidic arc") sources and close to average values for post-Archean average Australian Shale (PAAS; Taylor and McLennan, 1985), North American Shale Composite (NASC; Gromet *et al.*, 1984), and UCC (Figure 5). Several anchizone-grade and greenschist-facies banded metapsammitic samples display high Hf concentrations (Figure 5), defining a trend that possibly reflects derivation

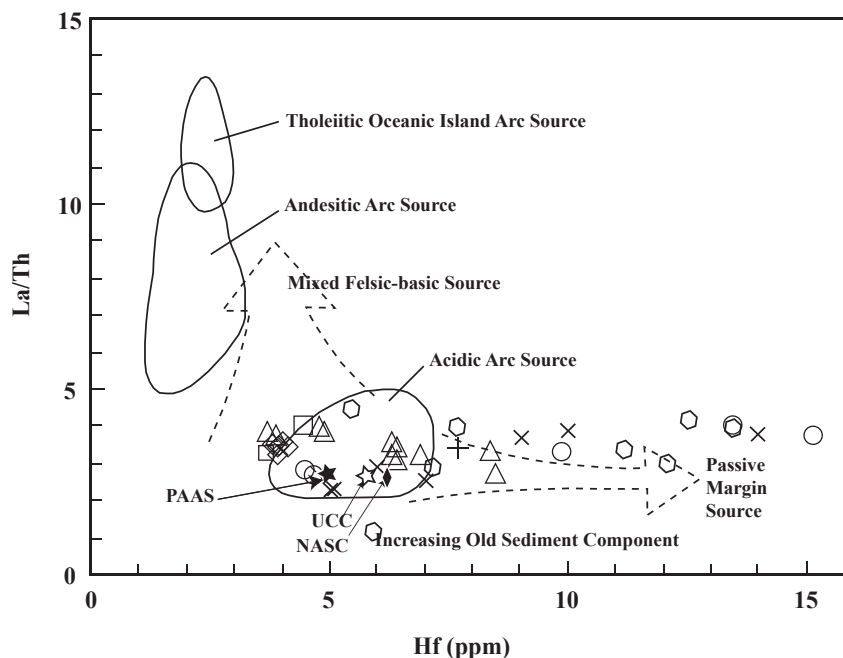


Figure 5. La/Th versus Hf tectonic setting discrimination plot (compositional fields after Floyd and Leveridge, 1987) for the Puncoviscana Fm. and higher-grade related metapsammitic rocks. Most samples reflect an acidic arc source, and plot around average upper continental crust compositions (UCC after McLennan *et al.*, 1990 and McLennan, 2001; marked with an empty star). Low-grade metapsammites show high Hf concentrations. PAAS, Post-Archean Australian Shales (after Taylor and McLennan, 1985; represented as a solid star); NASC, North American Shale Composite (after Gromet *et al.*, 1984; plotted as a solid diamond). The remaining symbols as in Figure 3.

from an old/recycled sediment component typical of passive margin sources or the progressive dissection of an arc.

The average concentration of total REE for our samples (average $\Sigma\text{REE} = 175$) is similar to PAAS (average $\Sigma\text{REE} = 181$; Taylor and McLennan, 1981) and higher than UCC values (average $\Sigma\text{REE} = 146$; McLennan, 2001). ΣREE values for anchizone-grade metapsammities are particularly high (average $\Sigma\text{REE} = 194$) compared to the rest of the samples (Table 2); anchizone and greenschist-grade metapsammitic samples generally show a higher HREE content than the rest of samples (Table 1).

Chondrite-normalized REE patterns for the analyzed samples are characterized by significant LREE enrichment, negative Eu anomalies, and relatively flat HREE (Figure 6), typical of upper crustal rocks (McLennan *et al.*, 1990). REE patterns are generally fractionated, with an average $(\text{La/Yb})_n$ value of 7.4 ± 1.15 . Anchizone-grade banded metapsammities exhibit the largest fractionation (average $(\text{La/Yb})_n = 8.46$; Table 2) and Tuclame banded metapsammities the lowest fractionation (average $(\text{La/Yb})_n = 6.37$; Table 2). $(\text{La/Sm})_n$ ratios range from 2.79–3.88 (average 3.43 ± 0.35) indicating some LREE fractionation (Table 1), which is largest in anchizone-grade banded metapsammities (average $(\text{La/Sm})_n = 3.79$; Table 2) and lowest in Tuclame banded metapsammities (average $(\text{La/Sm})_n = 2.92$; Table 2). $(\text{Gd/Yb})_n$ ratios vary between 1.11–1.77 (average 1.52 ± 0.16) consistent with nearly flat chondrite-normalized HREE patterns. Ce/Ce^* values are ~ 1 .

Our samples exhibit moderate to significant Eu/Eu^* anomalies (Table 1; Table 2), with values between 0.54 and 0.79 (average $\text{Eu/Eu}^* = 0.67$). 89% of the samples display $\text{Eu/Eu}^* > 0.6$, typical of source rocks affected by

intra-crustal differentiation processes and consistent with derivation from UCC sources (McLennan, 1989; McLennan *et al.*, 1990; McLennan, 2001).

5.3. Tectonic setting

The chemical composition of the source rock is a function of the tectonic setting, and exerts major control on the chemistry of sedimentary and metasedimentary rocks. Therefore, the geochemistry of sediments and metasedimentary rocks can be directly related to plate tectonic processes and has been traditionally used to identify their tectonic setting (Taylor and McLennan, 1985; Roser and Korsch, 1986; McLennan and Taylor, 1991). Trace elements, particularly those that are relatively immobile, with low residence times in seawater (*i.e.* La, Nd, Th, Zr, Hf, Nb, Ti) are reliable fingerprints for tectonic setting discrimination (McLennan *et al.*, 1990; Gu, 1996a, 1996b). On La–Th–Sc, Th–Co–Zr/10, and Th–Sc–Zr/10 plots (Bhatia and Crook, 1986; Figure 7), most data fall in the fields for “continental island-arc”. A group of anchizone and greenschist-facies banded metapsammitic samples plot in the “passive margin” field or between the “continental island arc” and “passive margin” fields.

La/Sc ratios are controlled by the mafic or felsic composition of the source: input from mafic and ultramafic source areas results in an enrichment of Sc. Additionally, Ti and Sc reflect the volcanic *vs.* mantelic compositional influence in the source. Zr and La provide information about the degree of recycling (McLennan *et al.*, 1990). Thus, Ti/Zr *vs.* La/Sc plots are helpful in the identification of the relative contribution of magmatic *vs.* recycled sources and

Table 2. Comparison of average ratios and total REE content in banded metapsammitic samples from the Puncoviscana Fm. and higher-grade related rocks with averages in sands from modern tectonic environments. Upper continental crust (UCC) ratios from McLennan, 2001.

Tectonic setting discriminators	(La/Yb) _n	(La/Sm) _n	(Gd/Yb) _n	Eu/Eu*	ΣREE
Passive Margin*	9.80	3.67	1.40	0.74	106.96
Back Arc Basin*	6.50	2.95	1.30	0.79	83.63
Continental Arc Basin*	7.18	3.19	1.30	0.76	113.49
Fore Arc Basin*	2.93	1.82	1.12	0.89	55.90
Fore Arc Basin ⁺	9.11	5.77	1.61	0.73	134.00
Ave. PVC Anc. metapsammities**	8.46	3.79	1.53	0.62	194.49
Ave. L-Grsch. Banded metapsammities**	7.40	3.39	1.54	0.70	144.77
Banded metapsammite from Sierra de Quilmes**	6.82	3.08	1.63	0.65	164.83
Ave. Ancasti Fm. banded metapsammities**	8.44	3.45	1.68	0.69	148.33
Ave. Tuclame Fm. Banded metapsammities**	6.37	2.92	1.58	0.69	125.09
UCC	9.21	4.20	1.40	0.65	146.37

Note. (*) average data from McLennan *et al.*, 1990; (+) average data from Mazur *et al.*, 2010

(**) average data from this research.

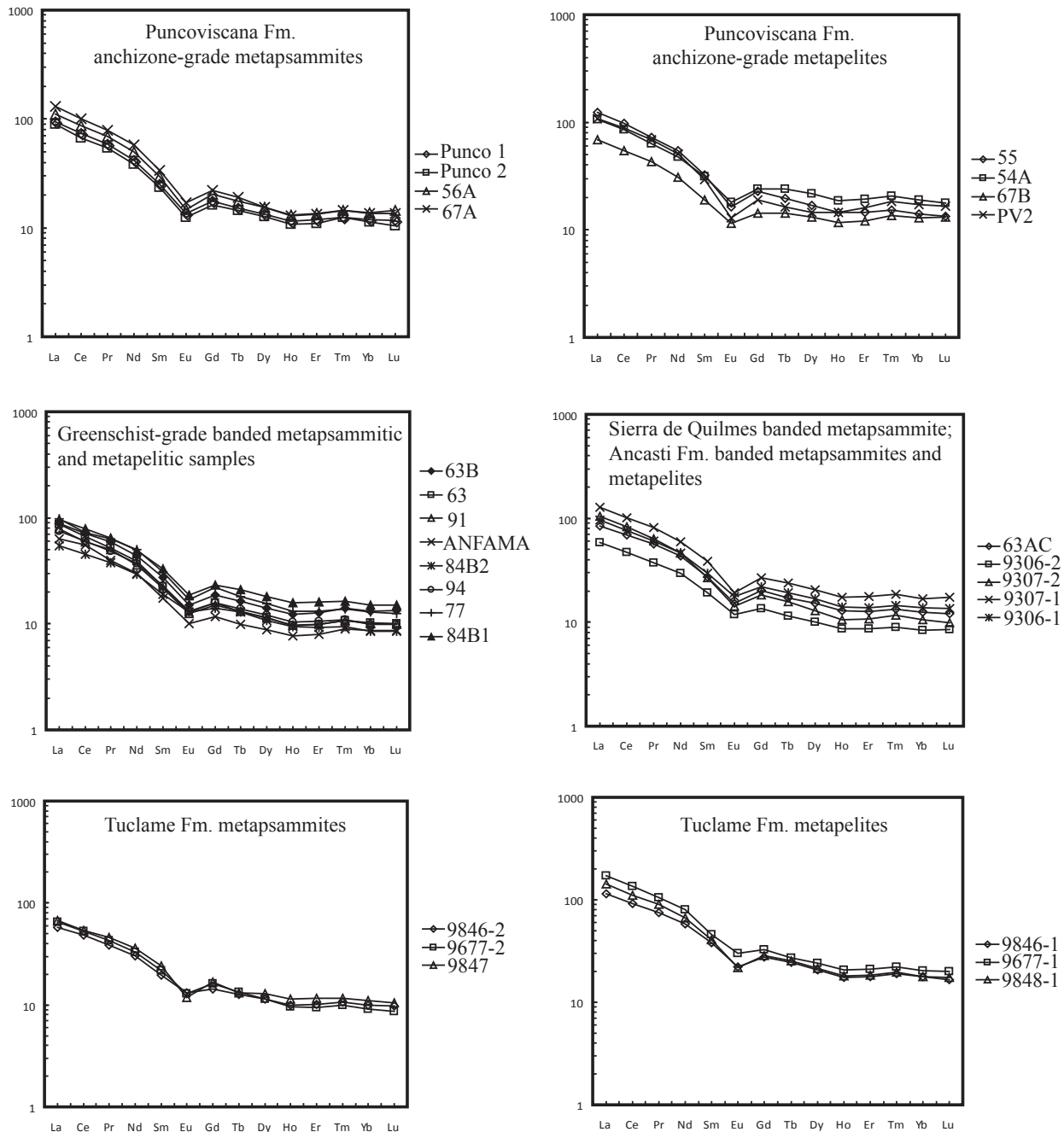


Figure 6. Chondrite-normalized REE patterns for the Puncoviscana Fm. and higher-grade related rocks. The patterns are similar to upper continental crust and post-Archean shales, with LREE enrichment, flat HREE, and significant negative Eu anomalies. Chondrite-normalizing factors from Taylor and McLennan (1985).

can discriminate successfully between different tectonic environments (Bhatia and Crook, 1986). In this diagram (Figure 8), most data plot in the fields for “active continental margin” and “continental island arc”. A group of anchizone and greenschist-facies banded metapsammitic samples plot in the “passive” margin field reflecting a higher input of recycled sources.

Upper continental crust-normalized multi-element

patterns are useful to discriminate the tectonic environment of greywackes (Floyd *et al.*, 1991). Figure 9 shows UCC-normalized patterns for average values calculated from our samples, and for sandstones from common tectonic environments (average data from Floyd *et al.*, 1991). Our samples show UCC-normalized patterns similar to those from continental arc/active margin and passive margin samples. A positive Ti-Hf-Zr-Y anomaly in our low-

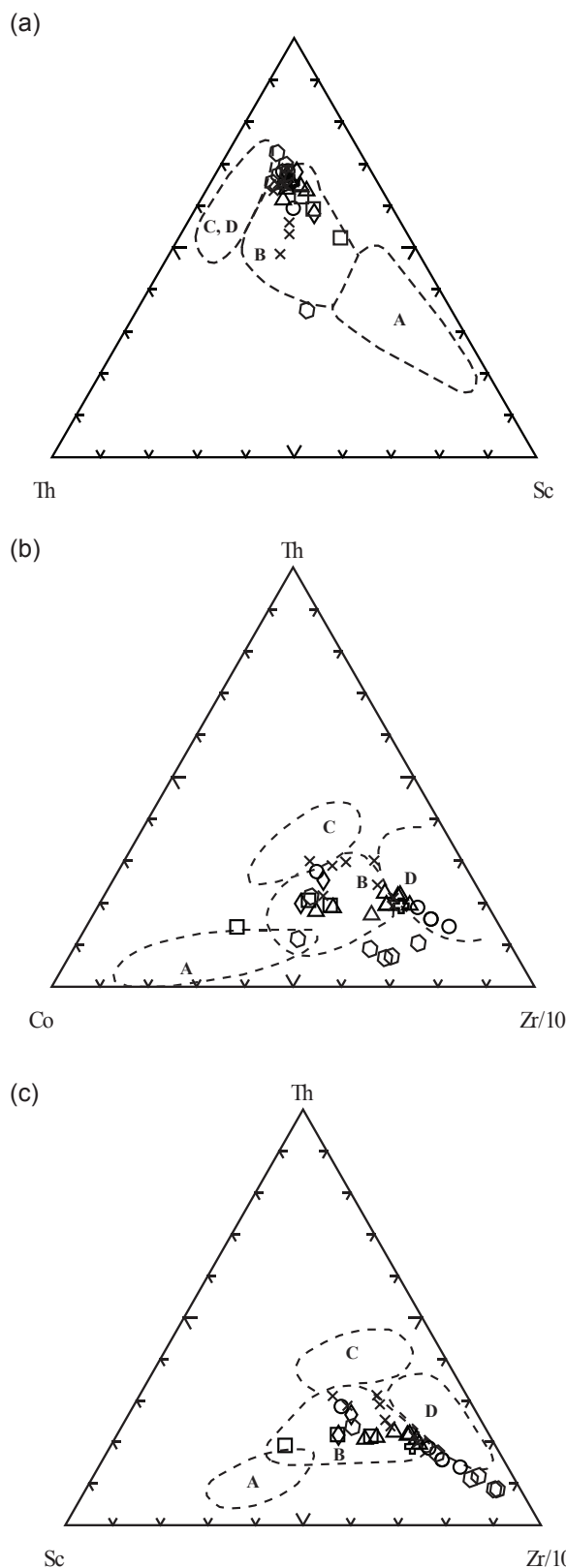


Figure 7. (a) La-Th-Sc, (b) Th-Co-Zr/10, and (c) Th-Sc-Zr/10 tectonic discrimination diagrams for the Puncoviscana Fm. and higher-grade related metapsammitic rocks. Dotted lines represent fields for sandstones from various tectonic settings (after Bhatia and Crook, 1986). A, oceanic island arc; B, continental island arc; C, active continental margin; D, passive margin. Symbols as in Figure 3.

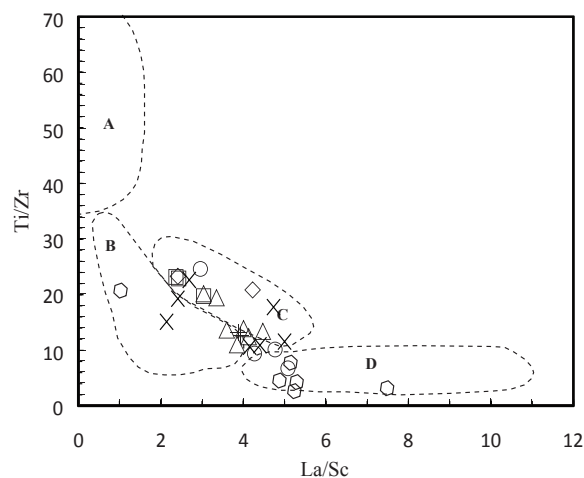


Figure 8. La/Sc vs. Ti/Zr tectonic discrimination diagram of the Puncoviscana Fm. and higher-grade related metapsammitic rocks. Dotted lines represent the fields for sandstones from various tectonic settings (after Bhatia and Crook, 1986). A, oceanic island arc; B, continental island arc; C, active continental margin; D, passive margin. Symbols as in Figure 3.

grade metapsammitic samples (Figure 9) likely reflects heavy mineral input (Floyd *et al.*, 1991). Negative Nb-Ta anomalies are characteristic of continental, passive margin, and subduction-related magmatic rocks (Hofmann, 1988; Floyd *et al.*, 1991). Nb-Ta anomalies are measured by the Nb/Nb* ratio, which is typically *c.* 0.15–0.30 for subduction-related rocks and *c.* 0.5 for passive margin sediments (Floyd *et al.*, 1991). Nb/Nb* ratios in our metapsammitic samples range from 0.24 to 0.4 and are consistent with sources related to subduction-related magmatic rocks.

In Table 3, sensitive discriminators of tectonic setting such as Th/Sc, Zr/Hf, La/Th, La/Sc, and Th/U ratios for the Puncoviscana Fm. and related rocks are compared to those for sandstones and greywackes from various tectonic settings (average values from Bhatia and Crook, 1986; McLennan *et al.*, 1990; Floyd and Leveridge, 1987; Mazur *et al.*, 2010). Average Th/Sc ratios in anchizone and greenschist-facies metapsammites are similar to those of trailing edge (passive margin), and dissected arc greywackes (McLennan *et al.*, 1990; Bhatia and Crook, 1986). Zr/Hf values in our samples are similar to those of “continental island arc”, and “dissected arc” greywackes. La/Th, La/Sc, and Th/U ratios in our samples are comparable with those of “continental arc” and “dissected arc” sandstones (Table 3).

(La/Yb)_n, (La/Sm)_n, (Gd/Yb)_n, and Eu/Eu* ratios, and Σ REE are sensitive discriminators of the tectonic setting (McLennan *et al.*, 1990). In Table 2 our samples show values for (La/Yb)_n, (La/Sm)_n, and Eu/Eu* similar to those of sediments from “continental arc basins” and “passive margins” (Table 2; McLennan *et al.*, 1990; McLennan, 2001). Eu anomalies in our samples are also typical for average UCC, recycled sedimentary rocks, and rocks from “differentiated continental volcanic arcs” dominated by felsic rocks that are exposed as the arc becomes dissected

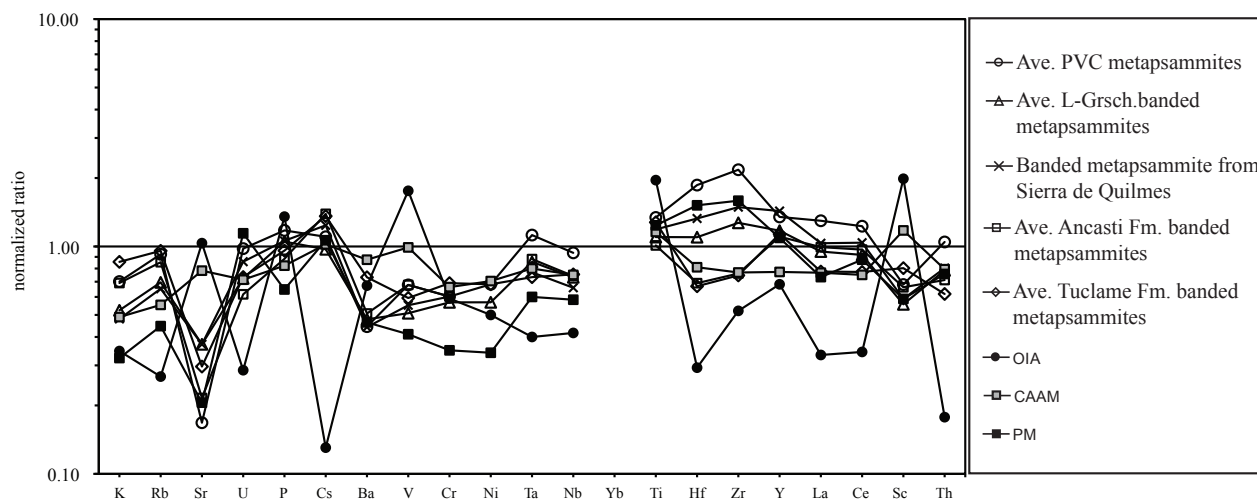


Figure 9. Upper continental crust normalized multi-element patterns for averaged greywacke data from different tectonic environments (from Floyd *et al.*, 1991). Also plotted are normalized average values for Puncoviscana Fm. and higher-grade related metapsammitic rocks (from this study). PVC, Anchizone-grade Puncoviscana Fm.; L-Grsch., Low-greenschist facies metaclastic rocks. OIA, oceanic island arc; CAAM, continental arc + active margin; PM, passive margin. Upper continental crust normalization values from Taylor and McLennan (1985), McLennan *et al.*, 1990, and McLennan, 2001. Puncoviscana Fm. and related samples display normalized patterns similar to those of CAAM and PM.

Table 3. Comparison of average ratios in Puncoviscana Fm. and higher-grade related rocks with averages in sands from modern tectonic environments. Upper continental crust (UCC) ratios from McLennan, 2001.

Tectonic setting discriminators	Continental Island Arc*	Active Continental Margin*	Fore Arc Basin+	Dissected Arc+	Trailing Edge**	Back Arc**	Fore Arc**	Continental Arc**	Ave. PVC Anc. metapsammites***	Ave. L-Grsch. Banded metapsammites***	Banded metapsammitite from Sierra de Quilmes***	Ave. Ancasti Fm. banded metapsammites***	Ave. Tuclame Fm. Banded metapsammites***	UCC
Th/Sc	0.85	2.59	1.37	1.10	1.08	0.51	0.09	0.75	1.23	1.11	1.08	0.85	0.66	0.79
Zr/Hf	36.30	26.30	34.88	34.99	30.96	33.81	31.38	28.03	38.06	37.78	36.75	36.17	36.55	32.75
La/Th	2.36	1.77	2.30	3.55	4.30	4.41	12.90	3.35	3.47	3.45	3.60	3.84	3.52	2.80
La/Sc	1.82	4.55	3.05	3.92	4.58	1.68	0.45	2.11	4.29	3.78	3.88	3.32	2.33	2.20
Th/U	4.60	4.80	3.02	3.51	3.22	3.21	1.80	3.53	4.11	4.11	3.58	4.39	3.23	3.82

Note: (*) average data from Bhatia and Crook, 1986; (+) average data from Floyd and Leveridge, 1987; (**) average data from McLennan *et al.*, 1990; (***) average data from this research.

(McLennan *et al.*, 1993).

6. Discussion

Our geochemical data show that the Puncoviscana Fm. and related metasedimentary rocks have chemical compositions that reflect enrichment in incompatible elements and depletion in some compatible elements compared to UCC (McLennan, 2001). Our data also suggest that the samples are derived from a moderately weathered, felsic source, in agreement with previously published data for the Puncoviscana Fm. (Do Campo and Ribeiro-Guevara, 2005; Zimmermann, 2005). According to results from tectonic discriminant diagrams, REE abundances, and UCC-normalized trace element patterns, our samples are characterized by a volcanic-arc signature. The interpretation of a volcanic arc derivation on the basis of the chemical composition of metasediments must be made cautiously, since it has been shown that specific tectonic settings do not necessarily produce rocks with unique geochemical signatures (McLennan *et al.*, 1990; Bahlburg, 1998), and

the continental crust itself is made of rocks bearing an arc-like composition (Bock *et al.*, 2000). However, the presence of volcanoclastic grains and felsic tuff beds in the Puncoviscana Fm. (Aparicio-González *et al.*, 2010; Jezek and Miller, 1987; Zimmermann, 2005; Escayola *et al.*, 2011) are also consistent with a volcanic arc source. Some authors describe the proportion of volcanoclastic grains as generally low (Jezek, 1990; Jezek and Miller, 1987; Zimmermann, 2005). This could be explained if most volcanic grains were weathered and dissolved to pseudomatrix (Zimmermann, 2005). Alternatively, if the source area was part of an evolved arc, denudation of volcanic levels and unroofing of the arc may have resulted in an increase of the proportion of sediments from exhumed plutonic and metasedimentary rocks, and the near absence of volcanic debris input into the basin. Recent studies based on detrital zircon ages from metasedimentary rocks of the Puncoviscana Fm. and higher-grade related rocks in Sierras de Cordoba, and ages obtained from syn- to post-kinematic granites suggest that at least part of the deposition of the sediments in the Puncoviscana basin was synchronous with a nearby Pampean magmatic arc (Escayola *et al.*, 2011; Iannizzotto *et al.*, 2013).

The Puncoviscana Fm. and low greenschist-facies metapsammitic samples display a chemical signature that suggests heavy mineral concentration and input of recycled sediments. This is consistent with their content of sedimentary and metamorphic lithoclasts and heavy minerals observed in thin section. In a La/Th vs. Hf plot, these samples show a trend to higher Hf contents, pointing to more recycled sources. This suggests a strong influence from old upper continental crust or recycled sedimentary rocks, as previously proposed by Do Campo and Ribeiro-Guevara (2005) for the Puncoviscana Fm. This recycled input could reflect either a deeper dissection of the arc source in the north, or a different source area with respect to the protoliths of metasedimentary rocks from Eastern Sierras Pampeanas. Nd isotope compositions and detrital zircon age maxima present in the very low- to low-grade Puncoviscana Fm. and related metaclastic rocks are similar to those in higher-grade metaclastic rocks of Eastern Sierras Pampeanas, suggesting related sources, or mixed sources with a similar TDM value (Drobe *et al.*, 2009; Collo *et al.*, 2009). Stronger reworking in northern areas of the basin could also explain the recycled component, but we would expect to observe higher degrees of alteration in our samples (higher CIA values). However, high silica concentration in metapsammitic samples can mask the alteration (e.g. Nesbitt and Young, 1982; Zimmermann, 2005). In a different scenario, the sediments filling the Puncoviscana basin may have been derived from source rocks with isotopic and geochemical signatures similar to those exhibited by Puncoviscana Fm. and related rocks; these source rocks may have been overlying the Rio de la Plata craton, and would be now completely eroded (Drobe *et al.*, 2011).

In tectonic discrimination diagrams using trace elements, metapsammitic samples mostly plot in the fields of continental island-arc, or active continental margin (Figures 7 and 8), while anchizone- and greenschist-facies metapsammitic samples plot in the passive margin field. Similar results were obtained by Escayola *et al.* (2011) for rocks from the Puncoviscana Fm. Trace element ratios traditionally considered as good indicators of the tectonic setting (Th/Sc, Zr/Hf, La/Th, La/Sc, and Th/U) in our low-grade metapsammitic samples are similar to those of sandstones from “passive margins” and “dissected arcs” (Tables 2 and 3).

Poorly sorted angular clasts in our low-grade metapsammitic samples, and the generally moderate degree of weathering observed in the Puncoviscana Fm. and related samples suggest rapid erosion and burial in a relatively close location to the source. This is compatible with dissected arc settings, characterized by rapid erosion rates and lower degrees of weathering compared to old upper crust (McLennan *et al.*, 1993). Eu/Eu* ratios and relatively high Hf content in low-grade metapsammitic samples are also consistent with dissected arcs (Floyd and Leveridge, 1987; McLennan *et al.*, 1993; Table 2). Based on petrographic analyses, Jezek (1990) previously suggested

a dissected volcanic arc source for the Puncoviscana Fm.

Detrital zircon age maxima from Puncoviscana Fm. and higher-grade related rocks suggest a mixing of late Neoproterozoic-Early Cambrian (520 - 650 Ma) and late Mesoproterozoic to early Neoproterozoic (~850 - 1150 Ma) sources (Rapela *et al.*, 1998; Adams *et al.*, 2010, 2011; Escayola *et al.*, 2007; Drobe *et al.*, 2011) that likely were relatively close to the Puncoviscana basin during sedimentation. The absence of detrital zircon maxima above 2 Ga and Nd model ages argues against the Rio de la Plata craton as a source for the metasediments of the Puncoviscana Fm. and higher-grade equivalents in Eastern Sierras Pampeanas (Schwartz and Gromet, 2004; Steenken *et al.*, 2006, 2010; Adams *et al.*, 2011; Escayola *et al.*, 2007; Rapela *et al.*, 2007; Drobe *et al.*, 2009 and references therein; Escayola *et al.*, 2011). Thus, a continental magmatic arc formed along the margin of a Mesoproterozoic craton during the Brasiliano orogeny may have been a potential source for the Puncoviscana Fm. and related rocks (Lucassen *et al.*, 2000; Steenken *et al.*, 2004; Escayola *et al.*, 2007; Schwartz and Gromet, 2004; Rapela *et al.*, 2007; Siegesmund *et al.*, 2009; Drobe *et al.*, 2009 and references therein). In recent works, the deposition of the Puncoviscana Fm. and related rocks would be coeval with the Pampean arc (Escayola *et al.*, 2011; Adams *et al.*, 2011; Iannizzotto *et al.*, 2013). Dominant magmatic and detrital sources from exhumed Mesoproterozoic basement and Brasiliano volcanic and plutonic rocks to the east of the Puncoviscana basin are consistent with volcanic arc geochemical signatures observed in our samples, with paleocurrent directions that indicate sediment transport from the east/southeast (Jezek and Miller, 1986; Jezek, 1990; Willner, 1990), and with detrital zircon ages obtained by other authors (Rapela *et al.*, 1998; Adams *et al.*, 2008a, 2008b; Escayola *et al.*, 2007; Drobe *et al.*, 2011).

Based on isotopic analysis, an extension of the Arequipa-Antofalla massif into the Sierras Pampeanas (Lucassen *et al.*, 2000; Steenken *et al.*, 2004; Escayola *et al.*, 2007; Collo *et al.*, 2009) or the Kalahari craton and its vicinity (Schwartz and Gromet, 2004; Rapela *et al.*, 2007; Siegesmund *et al.*, 2009; Drobe *et al.*, 2009 and references therein) have been proposed as a Mesoproterozoic source for the Puncoviscana and related metasedimentary rocks.

Collo *et al.* (2009) proposed a model in which the Puncoviscana Fm. and equivalent protoliths in Sierras Pampeanas likely were deposited as a back-arc sedimentary sequence that formed to the west of a continental Brasiliano volcanic arc developed on an extension of the Arequipa-Antofalla massif. This arc was related to west dipping subduction of oceanic crust under the Mesoproterozoic Arequipa-Antofalla terrane. Consistent with this model are geochemical signatures from volcanic rocks interlayered with metasedimentary rocks of the Puncoviscana Fm. that point to a rifting or a back-arc setting (Omarini *et al.*, 1999) and the volcanic arc geochemical signatures observed in our samples. A deeper dissection of the arc could have

contributed to the “recycled” and/or “heavy mineral” component observed in our low-grade samples.

In alternative models proposed by Rapela *et al.* (2007), Casquet *et al.* (2008), Drobe *et al.* (2009), Siegesmund *et al.* (2010) and references therein, the Puncoviscana Fm. was a fore-arc sedimentary sequence that developed on the margin of the Kalahari craton. In these models, the Puncoviscana Fm. and higher-grade equivalents were deposited in a basin to the west of a continental-arc source (*i.e.* Siegesmund *et al.*, 2009), also in agreement with the continental arc signature shown in this work, with the presence of volcanic detritus, poorly sorted angular clasts, rapid burial of the protoliths, and low CIA values of the samples. The composition of turbiditic deposits can vary among individual foreland basins from different settings (Caja *et al.*, 2010) and therefore their signature is widely variable. Th/Sc, Zr/Hf, La/Sc, (La/Yb)_n, (Gd/Yb)_n, and Eu/Eu* ratios, and Σ REE of our metapsammitic samples (Tables 2 and 3) are similar to those of turbiditic sandstones from a Carboniferous foreland basin in Western Poland (Mazur *et al.*, 2010). If the Puncoviscana Fm. turbiditic deposits and higher-grade equivalent metaclastic rocks represent the metasedimentary infill of a foreland basin, its detrital supply may have changed with time, mainly controlled by local tectonic processes and development of accommodation space in response to basin forming processes, as is common in foreland basin settings (Blair and Bilodeau, 1988; Haines *et al.*, 2001; McCann and Saintot, 2003; Maidment *et al.*, 2007). Based on the local presence of zircon maxima of ages around 520 Ma in lower-grade metaclastic rocks of the Puncoviscana Fm. (Adams *et al.*, 2008a) and on a previous model of Zimmermann (2005), Drobe *et al.* (2011) proposed a cannibalistic recycling model for the Puncoviscana Fm. Exhumation of deep crustal levels due to propagation of thrust belts in the foreland basin would provide sources for the recycled basin infill in shallow levels of the Puncoviscana basin and would account for the “recycled” signature observed in the low-grade metaclastic rocks.

The maximum age of sedimentation has been dated as 530 - 636 Ma (Lork *et al.*, 1990; Adams *et al.*, 2008a, 2008b) and *ca.* 537 Ma (Escayola *et al.*, 2011) in the Puncoviscana Fm., *ca.* 600 - 760 Ma in Sierras de Córdoba (Rapela *et al.*, 1998; Schwartz and Gromet, 2004; Escayola *et al.*, 2007), and 570 - 680 Ma in the Ancasti Fm. (Rapela *et al.*, 2007; Murra *et al.*, 2011). Based on detrital zircons and late-syn- or post-tectonic granitic intrusions, Escayola *et al.* (2011) constrained the Pampean deformation between *ca.* 537 and 524 Ma in northern localities of the Puncoviscana Fm. Metamorphic ages of the Pampean event have been determined as *ca.* 540 - 520 Ma in Sierras de Córdoba, (U/Pb zircon ages; Sims *et al.*, 1998; Rapela *et al.*, 1998). Intrusion of 536 - 520 Ma calc-alkaline syn- and post-tectonic granites in the low-grade folded Puncoviscana Fm. or the emplacement of the 530 ± 3 Ma calc-alkaline Sierra del Norte batholith (U-Pb zircon ages, Rapela *et al.*, 1998) in

folded metasedimentary rocks of Sierras de Córdoba further constrain the age of the Pampean deformation.

Despite local effects of a high-temperature Ordovician metamorphic event that becomes more prevalent to the south and west of the Pampean orogen (Figure 1) and Tertiary brittle deformation that locally overprints and completely reorients older structures, the style and sequence of structures and microstructures of the metasedimentary rocks remains consistent in all the studied localities: a compositional banding sub-parallel to bedding or relict bedding is folded into chevron structures (F_1) that are characterized by an associated fold-related cleavage (S_1) that is better developed with increasing metamorphic grade. The symmetric character of the folds, and their consistent geometry and trend, suggest that Pampean chevron folding and metamorphism were related to mainly orthogonal compression in the studied localities (Piñán-Llamas and Simpson, 2006). However, more recent structural studies in Sierras de Córdoba propose a compressive Early Cambrian deformational history that consists of a D1, characterized by folds with N-S to NE-SW trending axes and dextral mylonites, and a subsequent D2 with development of local dextral shear zones in some granites (von Gosen and Prozzi, 2010). Iannizzotto *et al.* (2013) suggest that dextral transpression was active at *c.* 537 Ma and was complete before 530 Ma in the Sierra del Norte batholith. Pampean deformation was likely due to east-dipping subduction along the western margin of the Puncoviscana basin, consistent with the presence of a NNE-trending series of Cambrian calc-alkaline granites to the east of the Puncoviscana Fm. (‘Pampean arc’ of Lira *et al.*, 1997; Rapela *et al.*, 1998; Siegesmund *et al.*, 2010 and references therein). In the Córdoba area, Pampean convergence ended with significant post-tectonic 515 - 520 Ma S-type peraluminous plutonism (*e.g.* Rapela *et al.*, 1998, 2002; Simpson *et al.*, 2003) that has been interpreted as related to eastward subduction of a mid-ocean ridge (Sims *et al.*, 1998; Gromet and Simpson, 1999; Siegesmund *et al.*, 2010 and references therein). This subduction likely ended with the collision and accretion of Western Sierras Pampeanas (Rapela *et al.*, 2007; Siegesmund *et al.*, 2010 and references therein). In a model proposed by Rapela *et al.* (2007), and references therein, this collision was followed by right-lateral shear movements that displaced the Pampean mobile belt to its present position adjacent to the Rio de la Plata craton. In alternative models, peraluminous magmatism in the Sierra de Córdoba was the result of the accretion of a para-autochthonous continental fragment, the Pampean Terrane, with the western margin of Gondwana (Rapela *et al.*, 1998). Ramos (2008 and references therein) considered that the Puncoviscana through was a peripheral foreland basin related to the collision of the Pampia block with the Rio de la Plata craton.

After the metamorphic peak, and during the mid- to Late Cambrian, the Pampean orogenic belt was rapidly exhumed, and eroded (Rapela *et al.*, 1998; Baldo *et al.*, 2006; Steenken

et al., 2011), serving as a probable source for the Mesón Group and adjacent peripheral basins to the west (Collo *et al.*, 2009; Drobe *et al.*, 2009, 2011). The uplifted Pampean terrane may have acted as a barrier, preventing Brasiliano and Mesoproterozoic sediments from reaching these basins (Collo *et al.*, 2009). Sediments in these basins were deformed, metamorphosed, and intruded by calc-alkaline magmatic complexes during the Famatinian cycle (490 - 460 Ma) due to east-dipping subduction of oceanic lithosphere beneath the western border of the Pampean belt (Pankhurst *et al.*, 1998, 2000; Saavedra *et al.*, 1998; Dahlquist *et al.*, 2008; Ducea *et al.*, 2010; Otamendi *et al.*, 2012).

7. Conclusions

1- Major and trace element geochemistry (*i.e.* Th/Sc, Rb/Sr, Cr/V, Cr/Th, Zr/Sc, Th/Sc, Eu/Eu*) indicates that the Puncoviscana Fm. and higher-grade related metaclastic rocks are characterized by moderate degrees of weathering (low CIA and high ICV values) and that metaclastic materials were likely derived from predominantly upper-crust felsic sources.

2- The overall geochemical fingerprints for all analyzed samples, including concentrations of La, Th, Sc, Zr, La/Sc, Nb/Nb*, and Eu/Eu* ratios, or UCC-normalized patterns, suggest that the Puncoviscana and related samples were deposited on a “continental island-arc” and (or) an “active continental margin” setting.

3- A heavy mineral/recycled signature, characterized by high Zr/Sc ratios and high concentrations of HREE, Hf, Ti, and Zr, is observed in low-grade psammitic samples. This signature, which is characteristic of passive margins or dissected arcs, could reflect the dissection of a continental arc source, a change in the source area, or a stage of stronger reworking within the depositional basin.

4- Diagnostic trace element ratios (Th/Sc, Zr/Hf, La/Th, La/Sc, Th/U, La_N/Yb_N , La_N/Sm_N , Gd_N/Yb_N), and large Eu anomalies, for the Puncoviscana Fm. and related rocks, are similar to those of sediments from modern continental arcs, continental island arc, and metasedimentary rocks related to dissected arcs.

5- Similarity in the style, orientation, and geometry of pre-Ordovician structures, and consistency in the sequence of deformation preserved in the Puncoviscana Fm. and higher-grade related rocks in the studied outcrops suggest a common deformation history during the Pampean orogeny.

6- Our results, in combination with previous geochronological, sedimentological, and isotopic data support a model in which the Puncoviscana and related sediments were deposited in a basin to the west of a Neoproterozoic Brasiliano or Pampean magmatic arc that formed along the margin of a Mesoproterozoic craton.

Acknowledgments

This research was partially financed through start-up funds to A.P.L.L. by Indiana University-Purdue University Fort Wayne and by the Gobierno Federal de México (Secretaría de Educación Pública) through a PROMEP grant UAEHGO-PTC-325 to J. E. C. This study benefited from the logistic help and discussions with José Pablo Lopez. We appreciate constructive reviews and comments made by Dr. Verdecchia and an anonymous reviewer.

References

- Aceñolaza, F.G., Toselli, A.J., 1973, Consideraciones estratigráficas y tectónicas sobre el Paleozoico inferior del Noroeste Argentino, *in* 2° Congreso Latinoamericano de Geología, Caracas, Venezuela: Caracas, Venezuela, Editorial Zucce, 2, 755-763.
- Aceñolaza, F.G., Durand, F.R., 1986, Upper Precambrian-lower Cambrian biota from the Northeast of Argentina: *Geological Magazine*, 123, 367-375.
- Aceñolaza, F.G., Miller, H., Toselli, A.J., 2002, Proterozoic–Early Paleozoic evolution in western South America – a discussion: *Tectonophysics*, 354, 121-137.
- Aceñolaza, F.G., Aceñolaza, G.F., 2005, La Formación Puncoviscana y unidades estratigráficas vinculadas en el Neoproterozoico – Cámbrico Temprano del Noroeste Argentino: *Latin American Journal of Sedimentology and Basin Analysis*, 12, 65–87.
- Adams, C.J., Miller, H., Toselli, A.J., Griffin, W.L., 2008a, The Puncoviscana Formation of northwest Argentina: U-Pb geochronology of detrital zircons and Rb-Sr metamorphic ages and their bearing on its stratigraphic age, sediment provenance and tectonic setting: *Neues Jahrbuch für Geologie und Paläontologie*, 247, 341-352.
- Adams, C.J., Miller, H., Toselli, A.J., 2008b, Detrital zircon U-Pb ages of the Puncoviscana Formation, Late Neoproterozoic–Early Cambrian, of NW Argentina: Provenance area and maximum age of deposition, *in* 6° South American Symposium on Isotope Geology, San Carlos de Bariloche, Río Negro, Argentina: Buenos Aires, INGEIS, 52.
- Adams, C.J., Miller, H., Aceñolaza, F.G., Toselli, A.J., Griffin, W.L., 2011, The Pacific Gondwana margin in the late Neoproterozoic–early Paleozoic: Detrital zircon U-Pb ages from metasediments in northwest Argentina reveal their maximum age, provenance and tectonic setting: *Gondwana Research*, 19, 71-83.
- Aparicio-González, P.A., Moya, M.C., Impiccini, A., 2010, Estratigrafía de las rocas metasedimentarias (Neoproterozoico–Cámbrico) de la Sierra de Mojotoro, Cordillera Oriental Argentina: *Latin American Journal of Sedimentology and Basin Analysis*, 17, 65-83.
- Astini, R.A., Ramos, V.A., Benedetto, J.L., Vaccari, N.E., Cañas, F.L., 1996, La Precordillera: Un terreno exótico a Gondwana, *in* XIII Congreso Geológico Argent y III Congreso de Exploración de Hidrocarburos, Buenos Aires, Argentina: Buenos Aires, Asociación Geológica Argentina, Actas 5, 293-324.
- Augustsson C., Rosing T., Adams, C.J., Chmiel, H., Kocabayoglu, M., Büld, M., Zimmermann, U., Berndt, J., Kooijman, E., 2011, Detrital Quartz and Zircon Combined: The Production of Mature Sand with Short Transportation Paths Along the Cambrian West Gondwana Margin, Northwestern Argentina: *Journal of Sedimentary Research*, 81, 284 - 298.
- Bachmann, G., Grauert, B., 1986, Isotopic dating of polymetamorphic metasediments from Northwest Argentina: *Zentralblatt für Geologie und Paläontologie*, 1, 1257-1268.

- Bachman, G., Grauert, B., Kramm, U., Lork, A., Miller, H., 1987, El magmatismo del Cámbrico Medio/Cámbrico Superior en el basamento del Noroeste argentino: investigaciones isotópicas y geocronológicas sobre los granitoides de los complejos intrusivos de Santa Rosa de Tástil y Cañaní, in X Congreso Geológico Argentino, Tucumán, Argentina: Tucumán, Sociedad Geológica Argentina, Actas 4, 125-127.
- Bahlburg H., 1998, The geochemistry and provenance of Ordovician turbidites in the Puna, in Pankhurst R.J., Rapela C.W. (eds.), The Proto-Andean margin of Gondwana: London, United Kingdom, Geological Society Special Publication, 142, 127-142.
- Bahlburg, H., Hervé, F., 1997, Geodynamic evolution and tectonostratigraphic terranes of northwestern Argentina and northern Chile: Bulletin of the Geological Society of America, 109, 869-884.
- Baldo, E.G., Casquet, C., Pankhurst, R.J., Galindo, C., Rapela, C.W., Fanning, C., Dahlquist, J., Murra, J., 2006, Neoproterozoic A-type magmatism in the Western Sierras Pampeanas (Argentina): evidence for Rodinia break-up along a proto-Iapetus rift?: Terra Nova, 18, 388-394.
- Becchio, R., Lucassen, F., Kaseman, S., Franz, G., Viramonte, J., 1999, Geoquímica y sistemática isotópica de rocas metamórficas del Paleozoico inferior. Noroeste de Argentina y Norte de Chile (21°-27°S): Acta Geológica Hispánica, 34, 273-299.
- Bhatia, M.R., Crook, K.A., 1986, Trace elements characteristics of greywackes and tectonic setting discrimination of sedimentary basins: Contributions to Mineralogy and Petrology, 92, 181-193.
- Blair, T.C., Bilodeau, W.W., 1988, Development of tectonic cyclothem in rift, pull-apart and foreland basins: Sedimentary response to episodic tectonism: Geology, 16, 517-520.
- Bock, B., Bahlburg, H., Worner, G., Zimmermann, U., 2000, Tracing crustal evolution in the Southern Central Andes from Late Precambrian to Permian with geochemical and Nd and Pb isotope data: Journal of Geology, 108, 515-535.
- Büttner, S., Glodny, J., Lucassen, F., Wemmer, K., Erdmann, S., Handler, R., Franz, G., 2005, Ordovician metamorphism and plutonism in the Sierra de Quilmes metamorphic complex: Implications for the tectonic setting of the northern Sierras Pampeanas (NW Argentina): Lithos, 83, 143-181.
- Caja, M.A., Marfil, R., García, D., Remacha, E., Morad, S., Mansurbeg, H., Amorosi, A., Martínez-Calvo, C., Lahoz-Beltrá, R., 2010, Provenance of siliciclastic and hybrid turbiditic arenites of the Eocene Hecho Group, Spanish Pyrenees: implications for the tectonic evolution of a foreland basin: Basin Research, 22, 157-180.
- Casquet, C., Pankhurst, R.J., Galindo, C., Rapela, C.W., Fanning, C.M., Baldo, E.G., Dahlquist, J., González-Casado, J.M., Colombo, F., 2008, A deformed alkaline igneous rock-carbonatite complex from the Western Sierras Pampeanas, Argentina: Evidence for late Neoproterozoic opening of the Clymene Ocean?: Precambrian Research, 165, 205-220.
- Coira, B.L., Barber, E., 1987, Vulcanismo submarino ordovícico (Arenigiano-Llanvirniano) del Río Huaiquitina, Provincia de Salta, Argentina, in X Congreso Geológico Argentino, Tucumán, Argentina: Tucumán, Argentina, Sociedad Geológica Argentina, 305-30.
- Coira, B.L., Manca, N., Chayle, W. E., 1990, Registros volcánicos en la Formación Puncoviscana, in Aceñolaza, F.G., Miller, H., Toselli, A.J. (eds.), El Ciclo Pampeano en el Noroeste Argentino, Serie Correlación Geológica: San Miguel de Tucumán, Argentina, Universidad Nacional de Tucumán, 4, 53-60.
- Collo, G., Astini, R.A., Cawood, P.A., Buchan, C., Pimentel, M., 2009, U-Pb detrital zircon ages and Sm-Nd isotopic features in low-grade metasedimentary rocks of the Famatina belt: implications for late Neoproterozoic-early Palaeozoic evolution of the proto-Andean margin of Gondwana: Journal of the Geological Society, London, 166, 303-319.
- Condie, K.C., 1991, Another look at rare earth elements in shales: Geochimica et Cosmochimica Acta, 55, 2527-2531.
- Condie, K.C., 1993, Chemical composition and evolution of the upper continental crust: Contrasting results from surface samples and shales: Chemical Geology, 104, 1-37.
- Cox, R., Low, D.R., Cullers, R.L., 1995, The influence of sediment recycling and basement composition on evolution of mudrock chemistry in the southwestern United States: Geochimica et Cosmochimica Acta, 59, 2919-2940.
- Cullers, R.L., 1994, The controls on the major and trace element variation of shales, siltstones, and sandstones of Pennsylvanian-Permian age from uplifted continental blocks in Colorado to platform sediment in Kansas, USA: Geochimica et Cosmochimica Acta, 58, 4955-4972.
- Dahlquist, J.A., Pankhurst, R.J., Rapela, C.W., Galindo, C., Alasino, P., Fanning, C.M., Saavedra, J., Baldo, E.G., 2008, New SHRIMP U-Pb data from the Famatina Complex: constraining Early-Mid Ordovician Famatinian magmatism in the Sierras Pampeanas, Argentina: Geologica Acta, 6, 319-333.
- Dahlquist, J.A., Rapela, C.W., Pankhurst, R.J., Fanning, C.M., Vervoort, J.D., Hart, G., Baldo, E. G., Murra, J.A., Alasino, P.H., Colombo, F., 2012, Age and magmatic evolution of the Famatinian granitic rocks of Sierra de Ancasti, Sierras Pampeanas, NW Argentina: Journal of South American Earth Sciences, 34, 10-25.
- Do Campo, M., Nieto, F., 2003, Transmission electron microscopy study of very low-grade metamorphic evolution in Neoproterozoic pelites of the Puncoviscana formation (Cordillera Oriental, NW Argentina): Clay Minerals, 38, 459-481.
- Do Campo, M., Ribeiro-Guevara, S.R., 2002, Geoquímica de las secuencias clásticas de la Formación Puncoviscana (Neoproterozoico, NO Argentina), proveniencia y marco tectónico, in XV Congreso Geológico Argentino, El Calafate, Argentina: Buenos Aires, Sociedad Geológica Argentina, disponible en CD.
- Do Campo, M., Ribeiro-Guevara, S.R., 2005, Provenance analysis and tectonic setting of late Neoproterozoic metasedimentary successions in NW Argentina: Journal of South American Earth Sciences, 19, 143-153.
- Drobe, M., López de Luchi, M.G., Steenken, A., Frei, R., Naumann, R., Wemmer, K., Siegesmund, S., 2009, Provenance of the late Proterozoic to early Cambrian metaclastic sediments of the Sierra de San Luis (Eastern Sierras Pampeanas) and Cordillera Oriental, Argentina: Journal of South American Earth Sciences, 28, 239-262.
- Drobe, M., López de Luchi, M., Steenken, A., Wemmer, K., Naumann, R., Frei, R., Siegesmund, S., 2011, Geodynamic evolution of the Eastern Sierras Pampeanas (Central Argentina) based on geochemical, Sm-Nd, Pb-Pb and SHRIMP data: International Journal of Earth Sciences, 100, 631-657.
- Ducea, M.N., Otamendi, J.E., Bergantz, G., Stair, K., Valencia, V., Gehrels, G., 2010, Timing constraints on building an intermediate plutonic arc crustal section: U-Pb zircon geochronology of the Sierra Valle Fértil, Famatinian Arc, Argentina: Tectonics, 29, TC4002, doi:10.1029/2009TC002615.
- Durand, F.R., 1996, La transición Precámbrico-Cámbrico en el sur de Sudamérica, in Baldi, B., Aceñolaza, F. (eds), Early Paleozoic evolution in NW Gondwana: Universidad Nacional de Tucumán, Argentina, Serie Correlación Geológica, 12, 195-205.
- Escayola, M.P., Pimentel, M.M., Armstrong, M., 2007, Neoproterozoic backarc basin: Sensitive high-resolution ion microprobe U-Pb and Sm-Nd isotopic evidence from the Eastern Pampean Ranges, Argentina: Geology, 35, 495-498.
- Escayola, M.P., van Staal, C.R., Davis, W.J., 2011, The age and tectonic setting of the Puncoviscana Formation in northwestern Argentina: an accretionary complex related to Early Cambrian closure of the Puncoviscana Ocean and accretion of the Arequipa-Antofalla block: Journal of South American Earth Sciences, 32, 438-459.
- Fantini, R., Gromet, P., Simpson, C., Northrup, C.J., 1998, Timing of high-temperature metamorphism in the Sierras Pampeanas of Córdoba, Argentina: implications for a Laurentia-Gondwana Interactions, in X Congreso Latinoamericano de Geología y VI Congreso Nacional de Geología Económica, Buenos Aires, Argentina: Buenos Aires, Argentina, Sociedad Geológica Argentina, Actas II, 388-392.

- Fedo, C.M., Nesbitt, H.W., Young, G.M., 1995, Unraveling the effects of potassium metasomatism in sedimentary rocks and paleosols, with implications for paleoweathering conditions and provenance: *Geology*, 23, 921-924.
- Fedo, C.M., Eriksson, K.A., Krogstad, E.J., 1996, Geochemistry of shales from the Archean (~3.0 Ga) Buhwa Greenstone Belt, Zimbabwe: implications for provenance and source-area weathering: *Geochimica et Cosmochimica Acta*, 60, 1751-1763.
- Floyd, P.A., Leveridge, B.E., 1987, Tectonic environment of the Devonian Gramscatho basin, south Cornwall: framework mode and geochemical evidence from turbiditic sandstones: *Journal of the Geological Society*, 144, 531-542.
- Floyd, P.A., Shail, R., Leveridge, B. E., Franke, W., 1991, Geochemistry and provenance of Rhenohercynian synorogenic sandstones: implications for tectonic environment discrimination, in Morton, A.C., Todd, S.P., Haughton, P.D.W. (eds.), *Developments in Sedimentary Provenance Studies*, Special Publication: London, United Kingdom, *Journal of the Geological Society of London*, 57, 173-188.
- García, D., Fontelles, M., Moutte, J., 1994, Sedimentary fractionations between Al, Ti, and Zr and the genesis of strongly prealuminous granites: *Journal of Geology*, 102, 411-422.
- Girty, G.H., Hanson, A.D., Knaack, C., Johnson, D., 1994, Provenance determined by REE, Th, and Sc analyses of metasedimentary rocks, Boyden Cave roof pendant, central Sierra Nevada, California: *Journal of Sedimentary Research*, 64, 68-73.
- González, O. E., Viruel, M. E., Mon, R., Tchilinguirian, P., Barber, E., 2000, Hoja Geológica 2766-II San Miguel de Tucumán, escala 1:250000, Buenos Aires, Argentina, Servicio Geológico Argentino, Programa Nacional de Cartas Geológicas de la República Argentina, 1 mapa, Boletín 245.
- Gosen, W. von, Prozzi, C., 2010, Pampean deformation in the Sierra Norte de Córdoba, Argentina: Implications for the collisional history at the western pre-Andean Gondwana margin, *Tectonics*, 29, TC2012, doi: 10.1029/2009TC002580.
- Gromet, L.P., Dymek, R.R., Haskin, L.A., Korotev, R.L., 1984, The "North American Shale Composite": Its compilation, major, and trace element characteristics: *Geochimica et Cosmochimica Acta*, 48, 2469-2482.
- Gromet, L.P., Simpson, C., 1999, Age of the Paso del Carmen pluton and implications for the duration of the Pampean Orogeny, Sierras de Córdoba, Argentina, in XIV° Congreso Geológico Argentino, Salta, Argentina: Salta, Argentina, Víctor Manuel Hanne, 14, 149-151.
- Gromet, L.P., Simpson, C., 2000, Cambrian orogeny in the Sierras Pampeanas, Argentina: ridge subduction or continental collision?, in *Geological Society of America Annual Meeting*, Reno, Nevada: Boulder, Colorado, Geological Society of America, Abstracts with Programs, 32, A450.
- Gu X.X., 1996a, Geochemical characteristics of sediments and tectonic setting analysis of sedimentary basins, in *Developments in Geosciences and Technology*, 1995. Press of the University of Geosciences of China, Beijing, 205-212.
- Gu, X.X., 1996b, Geochemical characteristics of the Triassic Tethys sediments in NW-Sichuan and its implications to the weathering conditions in source regions: *Mineral Petrology and Geochemistry Bulletin*, 15, 23-27.
- Haines, P.W., Hand, M., Sandiford, M., 2001, Paleozoic synorogenic sedimentation in central and northern Australia: a review of distribution and timing with implications for the evolution of intercontinental orogens: *Australian Journal of Earth Sciences*, 48, 911-928.
- Hauser, N., Matteini, M., Omarini, R.H., Pimentel, M.M., 2011, Combined U-Pb and Lu-Hf isotope data on turbidites of the Paleozoic basement of NW Argentina and petrology of associated igneous rocks: Implications for the tectonic evolution of western Gondwana between 560 and 460 Ma: *Gondwana Research*, 19, 100-127.
- Hofmann, A.W., 1988, Chemical differentiation of the Earth: the relationship between mantle, continental crust, and oceanic crust: *Earth and Planetary Science Letters*, 90, 297-314.
- Iannizzotto, N.F., Rapela, C.W. Baldo, E. G.A. Galindo, C., Fanning, C.M., Pankhurst, R.J., 2013, The Sierra Norte-Ambargasta batholith: Late Ediacaran-Early Cambrian magmatism associated with Pampean transpressional tectonics: *Journal of South American Earth Sciences*, v. 42, 127-143.
- Jezek, P., 1990, Análisis sedimentológico de la Formación Puncoviscana entre Tucumán y Salta, in Aceñolaza, F.G., Miller, H., Toselli, A.J. (eds.), *El Ciclo Pampeano en el Noroeste Argentino, Serie Correlación Geológica: San Miguel de Tucumán, Argentina*, Universidad Nacional de Tucumán, 9-36.
- Jezek, P., Miller, H., 1986, Deposition and facies distribution of turbiditic sediments of the Puncoviscana Formation (Upper Precambrian-lower Cambrian) within the basement of the NW Argentine Andes: *Zentralblatt für Geologie und Paläontologie*, 9-10, 1235-1244.
- Jezek, P., Miller, H., 1987, Petrology and facies analysis of turbiditic sedimentary rocks of the Puncoviscana through (Upper Precambrian-lower Cambrian) in the basement of the NW Argentine Andes, in Garry D. McKenzie, (ed.) *Gondwana Six: Structure, tectonics, and geophysics*: Washington, D.C., U.S.A., Geophysical Monograph, 287-293.
- Jezek, P., Willner, A.P., Aceñolaza, F.G., Miller, H., 1985, The Puncoviscana trough - a large basin of Late Precambrian to Early Cambrian age on the Pacific edge of the Brazilian shield: *Geologische Rundschau*, 74, 573-584.
- Jordan, T.E., Allmendinger, R.W., 1986, The Sierras Pampeanas of Argentina: a modern analogue of Rocky Mountain foreland deformation: *American Journal of Science*, 286, 737-764.
- Krol, M.A., Simpson, C., 1999, Thermal history of the eastern Sierras Pampeanas accretionary prism rocks, constraints from ⁴⁰Ar/³⁹Ar mica data, in *Geological Society of America Annual Meeting*, Denver, Colorado, Abstracts with Programs: Boulder, Colorado, U.S.A., Geological Society of America, 31, 114-115.
- Li, Q., Liu, S., Han, B., Zhang, J., Chu, Z., 2005, Geochemistry of metasedimentary rocks of the Proterozoic Xingxingxia complex: implications for provenance and tectonic setting of the eastern segment of the Central Tianshan Tectonic Zone, northwestern China: *Canadian Journal of Earth Sciences*, 42, 287-306.
- Lira, R., Millone, H. A., Kirschbaum, A.M., Moreno, R.S., 1997, Calc-alkaline arc granitoid activity in the Sierra Norte-Ambargasta Ranges, Central Argentina: *Journal of South American Earth Sciences*, 10, 157-177.
- Lork, A., Miller, H., Kramm, U., Grauert, B., 1990, Sistemática U-Pb de circones detríticos de la Formación Puncoviscana y su significado para la edad máxima de sedimentación en la Sierra de Cachi (Provincia de Salta, Argentina), in Aceñolaza, F.G., Miller, H., Toselli, A.J. (eds.), *El Ciclo Pampeano en el Noroeste Argentino, Serie Correlación Geológica: San Miguel de Tucumán, Argentina*, Universidad Nacional de Tucumán, 4, 199-208.
- Lucassen, F., Becchio, R., Wilke, H.G., Franz, G., Thirlwall, M.F., Viramonte, J., Wemmer, K., 2000, Proterozoic -Paleozoic development on the basement of the Central Andes (18-26°S) - a mobile belt of the South America craton: *Journal of South American Earth Sciences*, 13, 697-715.
- Maidment, D.W., Williams, I.S., Hand, M., 2007, Testing long-term patterns of basin sedimentation by detrital zircon geochronology, Centralian superbasin, Australia: *Basin Research*, 19, 335-360.
- Mazur, S., Aleksandrowski, P., Turniak, K., Krzeminski, L., Mastalerz, K., Górecka-Nowak, A., Kurowski, L., Krzywiec, P., Zelazniewicz, A., Fanning, M.C., 2010, Uplift and late orogenic deformation of the Central European Variscan belt as revealed by sediment provenance and structural record in the Carboniferous foreland basin of western Poland: *International Journal of Earth Sciences (Geologische Rundschau)*, 99, 47-64.
- McCann, T., Saintot, A., 2003, Tracing tectonic deformation using the sedimentary record: an overview, in McCann, Saintot, A. (eds.), *Tracing tectonic deformation using the sedimentary record*: London, United Kingdom, Geological Society of London, Special Publication, 208, 1-28.

- McLennan, S.M., 1989, Rare earth elements in sedimentary rocks: influence of provenance and sedimentary processes: *Reviews in Mineralogy*, 21, 169-200.
- McLennan, S.M., 2001, Relationships between the trace element composition of sedimentary rocks and upper continental crust: *Geochemistry Geophysics Geosystems*, 2, 1021-1045.
- McLennan, S.M., Taylor S.R., 1991, Sedimentary rocks and crustal evolution: tectonic setting and secular trends: *Journal of Geology*, 99, 1-21.
- McLennan, S.M., Taylor, S.R., Eriksson, K.A., 1983, Geochemistry of Archean shales from the Pilbara Supergroup, Western Australia: *Geochimica et Cosmochimica Acta*, 47, 1211-1222.
- McLennan, S.M., Taylor, S.R., McCulloch, M.T., Maynard, J.B., 1990, Geochemical and Nd-Sr isotopic composition of deep-sea turbidites: crustal evolution and plate tectonic associations: *Geochimica et Cosmochimica Acta*, 54, 2015-2050.
- McLennan, S.M., Hemming, S., McDaniel, D.K., Hanson, G.N., 1993, Geochemical approaches to sedimentation, provenance and tectonics, in Johnsson, M.J., Basu, A. (eds.), *Processes controlling the composition of clastic sediments*, Geological Society of America Special Publications: Boulder, Colorado, U.S.A., Geological Society of America, 284, 21-40.
- McLennan, S.M., Hemming, S. R., Taylor, S.R., Eriksson, K.A., 1995, Early Proterozoic crustal evolution: geochemical and Nd-Pb isotopic evidence from metasedimentary rocks, southwestern North America: *Geochimica et Cosmochimica Acta*, 59, 1153-1177.
- Meinhold, G., Kostopoulos, D., Reischmann, T., 2007, Geochemical constraints on the provenance and depositional setting of sedimentary rocks from the islands of Chios, Inousses, and Psara, Aegean Sea, Greece: Implications for the evolution of Palaeotethys: *Journal of the Geological Society*, London, 164, 1145-1163.
- Mon, R., Hongn, F.D., 1991, The structure of the Precambrian and lower Paleozoic basement of the Central Andes between 22° and 32°S Lat.: *Geologische Rundschau*, 80, 745-758.
- Murra, J., Baldo, E., Galindo, C., Casquet, C., Pankhurst, R., Rapela, C., Dahlquist, J., 2011, Sr and O isotope composition of marbles from the Sierra de Ancasti, Eastern Sierras Pampeanas, Argentina: age and constraints for the Neoproterozoic-lower Paleozoic evolution of the proto-Gondwana margin: *Geologica Acta*, 9, 79-92.
- Nesbitt, H.W., Young, G.M., 1982, Early Proterozoic climates and plate motions inferred from major element chemistry of lutites: *Nature*, 299, 715-717.
- Nesbitt, H.W., Young, G.M., 1984, Prediction of some weathering trends of plutonic and volcanic rocks based on thermodynamic and kinetic considerations: *Geochimica et Cosmochimica Acta*, 48, 1523-1534.
- Nesbitt, H.W., Young, G.M., 1989, Formation and diagenesis of weathering profiles: *Journal of Geology*, 97, 129-147.
- Omarini, R.H., Sureda, R.J., Gotze, H.J., Seilacher, A., Pfluger, F., 1999, Puncoviscana folded belt in northwestern Argentina: testimony of Late Proterozoic Rodinia fragmentation and pre-Gondwana collisional episodes: *International Journal of Earth Sciences*, 88, 76-97.
- Otamendi, J.E., Ducea, M.N., Bergantz, G.W., 2012, Geological, Petrological, and Geochemical Evidence for Progressive Construction of an Arc Crustal Section, Sierra de Valle Fértil, Famatinian Arc, Argentina: *Journal of Petrology*, 53, 4.
- Pankhurst, R.J., Rapela, C.W., Saavedra, J., 1997, The Sierras Pampeanas of NW Argentina-growth of the Pre-Andean margin of Gondwana: *European Union of Geosciences, Abstract Supplement I, Terra Nova*, 9, 1-162.
- Pankhurst, R.J., Rapela, C.W., Saavedra, J., Baldo, E., Dahlquist, J., Pascua, I., Fanning, C.M., 1998, The Famatinian magmatic arc in the central Sierras Pampeanas: an Early to Mid-Ordovician continental arc on the Gondwana margin, in Pankhurst R.J., Rapela, C.W. (eds.), *The proto-Andean Margin of Gondwana*: London, United Kingdom, Special Publication of the Geological Society of London, 142, 343-367.
- Pankhurst, R.J. Rapela, C.W. & Fanning, C.M., 2000, Age and origin of coeval TTG, I- and S-type granites in the Famatinian belt of NW Argentina: *Transactions of the Royal Society of Edinburgh: Earth Science*, 91, 151-168.
- Piñán-Llamas, A., Simpson, C., 2006, Deformation of Gondwana margin turbidites during the Pampean orogeny, north-central Argentina: *Geological Society of America Bulletin*, 118, 1270-1279.
- Piñán-Llamas, A., Simpson, C., 2009, Primary structure influence on compositional banding in psammites: Examples from the Puncoviscana Formation, North-central Argentina: *Journal of Structural Geology*, 31, 55-71.
- Porto, J.C., Fernández, R.I., Carrión, M.H., 1990, Calizas y dolomías de la Formación Puncoviscana, in Aceñolaza, F.G., Miller, H., Toselli, A.J. (eds.), *El Ciclo Pampeano en el Noroeste Argentino, Serie Correlación Geológica*: San Miguel de Tucumán, Argentina, Universidad Nacional de Tucumán, 4, 37-52.
- Ramos, V.A., 1988, Late Proterozoic-Early Paleozoic of South America - a Collisional History: *Episodes*, 11, 168-174.
- Ramos, V., 1999, Las provincias geológicas del territorio argentino, in Caminos, R. (ed.), *Geología Argentina*: Buenos Aires, Argentina, Servicio Geológico-Minero Argentino, Anales 29, 41-96.
- Ramos, V.A., 2008, The basement of the Central Andes: the Arequipa and related Terranes: *Annual Review of Earth and Planetary Sciences*, 36, 289-324.
- Ramos, V.A., 2009, Anatomy and global context of the Andes: Main geologic features and the Andean orogenic cycle, in Kay, S.M., Ramos, V.A., Dickinson, W.R., (eds.), *Backbone of the Americas: Shallow Subduction, Plateau Uplift, and Ridge and Terrane Collision*: Boulder, Colorado, U.S.A., Geological Society of America, Memoir 204, 31-65.
- Ramos, V.A., Jordan, T.E., Allmendinger, R.W. Mpodozis, C., Kay, S.M., Cortes, J. M., Palma, M., 1986, Paleozoic terranes of the central Argentine-Chilean Andes: *Tectonics*, 5, 855-880.
- Ramos, V.A., Escayola, M., Mutt, D.I., Vujovich, G.I., 2000, Proterozoic-early Paleozoic ophiolites of the Andean basement of southern South America, in Dilek, Y., Moores, E.M., Elthon, D., Nicolas, A. (eds.), *Ophiolites and oceanic crust: new insights from field studies and the Ocean Drilling Program*: Boulder, Colorado, U.S.A., Geological Society of America, Special Paper, 349, 331-349.
- Ramos, V.A., Cristallini, E.O., Perez, D.J., 2002, The Pampean flat-slab of the Central Andes: *Journal of South American Earth Sciences*, 15, 59-78.
- Rapela, C.W., Pankhurst, R.J., Casquet, C., Baldo, E.G., Saavedra, J., Galindo, C., Fanning, C. M., 1998, The Pampean Orogeny of the south proto-Andes: evidence for Cambrian continental collision in the Sierras de Córdoba, in Pankhurst, R.J., Rapela, C.W. (eds.), *The proto-Andean Margin of Gondwana*: London, United Kingdom, Special Publication of the Geological Society, 142, 181-217.
- Rapela, C.W., Toselli, A., Heaman, L., Saavedra, L., 1990, Granite plutonism of the Sierras Pampeanas; an inner eordilleran Palaeozoic arc in the southern Andes, in May, S.M., Wela, C.W. (eds.), *Plutonism from Antarctica to Alaska*: Boulder, Colorado, U.S.A., Geological Society of America Special Paper, 241, 77-99.
- Rapela, C.W., Baldo, E.G., Pankhurst, R.J., Saavedra, J., 2002, Cordierite and Leucogranite Formation during Emplacement of Highly Peraluminous Magma: the El Pilón Granite Complex (Sierras Pampeanas, Argentina): *Journal of Petrology*, 43, 1003-1028.
- Rapela, C.W., Pankhurst, R. J., Casquet, C., Fanning, C.M., Baldo, E.G., Gonzales-Casado J.M., Galindo, C., Dahlquist, J., 2007, The Rio de la Plata craton and the assembly of SW Gondwana: *Earth Sciences Review*, 83, 49-82.
- Roser, B.P., Korsch, R.J., 1985, Plate tectonics and geochemical composition of sandstones: A discussion: *Journal of Geology*, 93, 81-84.
- Roser, B.P., Korsch, R.J., 1986, Determination of tectonic setting of sandstone-mudstone suites using SiO₂ content and K₂O/Na₂O ratio: *Journal of Geology*, 94, 635-650.
- Roser, B.P., Korsch, R.J., 1988, Provenance signatures of sandstone-mudstone suites determined using discriminant function analysis of major-element data: *Chemical Geology*, 67, 119-139.

- Roser, B.P., Cooper, R.A., Nathan, S., Tulloch, A.J., 1996, Reconnaissance sandstone geochemistry, provenance, and tectonic setting of the lower Paleozoic terranes of the West Coast and Nelson, New Zealand: *Journal of Geology and Geophysics*, 39, 1-16.
- Saavedra, J., Toselli, A., Rossi, J., Pellitero, E., Durand, F., 1998, The Early Paleozoic magmatic record of the Famatina System: a review, *in* Pankhurst, R.J., Rapela, C.W. (eds.), *The proto-Andean Margin of Gondwana*: London, United Kingdom, Special Publications of the Geological Society, 142, 283-295.
- Sánchez, M.C., Salfity, J.A., 1999, La cuenca cámbrica del Grupo Mesón en el noroeste argentino: Desarrollo estratigráfico y paleogeográfico: *Acta Geológica Hispánica*, 34, 123-139.
- Schwartz, J.J., Gromet, L.P., 2004, Provenance of a late Proterozoic-early Cambrian basin Sierras de Córdoba, Argentina: *Precambrian Research*, 129, 1-21.
- Schwartz, J.J., Gromet, L.P., Miró, R., 2008, Timing and duration of the calc-alkaline arc of the Pampean Orogeny: implications for the Late Neoproterozoic to Cambrian evolution of Western Gondwana: *Journal of Geology*, 116, 39-61.
- Shaw, D.M., 1968, A review of K-Rb fractionation trends by covariance analysis: *Geochimica et Cosmochimica Acta*, 32, 573-601.
- Siegesmund, S., Steenken, A., Martino, R.D., Wemmer, K., Lopez de Luchi, M., Frei, R., Presnyakov, S., Guerreschi, A., 2010, Time constraints on the tectonic evolution of the Eastern Sierras Pampeanas (Central Argentina): *International Journal of Earth Sciences*, 99, 1199-1226.
- Simpson, C., Law, R.D.W., Gromet, L.P., Miro, R., Northrup, C.J., 2003, Paleozoic deformation in the Sierras de Córdoba and Sierra de Las Minas, eastern Sierras Pampeanas, Argentina: *Journal of South American Earth Sciences*, 15, 749-764.
- Sims, J.P., Ireland, T.R., Camacho, A., Lyons, P., Pieters, P.E., Skirrow, R.G., Stuart-Smith, P.G., Miró, R., 1998 U-Pb, Th-Pb, and Ar-Ar geochronology from the southern Sierras Pampeanas, Argentina: implications for the Palaeozoic tectonic evolution of the western Gondwana margin, *in* Pankhurst, R.J., Rapela, C.W. (eds.), *The proto-Andean Margin of Gondwana*: London, United Kingdom, Special Publications of the Geological Society, London, 142, 259-281.
- Steenken, A., López de Luchi, M.G., Siegesmund, S., Wemmer, K., Pawlig, S., 2004, Crustal provenance and cooling of the basement complexes of the Sierra de San Luis: an insight into the tectonic history of the proto-Andean margin of Gondwana: *Gondwana Research*, 7, 1171-1195.
- Steenken A., Siegesmund S., López de Luchi M.G., Frei R., Wemmer K., 2006, Neoproterozoic to Early Palaeozoic events in the Sierra de San Luis: implications for the Famatinian geodynamics in the Eastern Sierras Pampeanas (Argentina): *Journal of the Geological Society*, 163, 965-982.
- Steenken, A., Wemmer, K., Martino, R.D., López de Luchi, M.G., Guerreschi, A., Siegesmund, S., 2010, Post-Pampean cooling and the uplift of the Sierras Pampeanas in the west of Córdoba (Central Argentina): *Neues Jahrbuch für Geologie und Paläontologie*, 256, 235-255.
- Steenken, A., López de Luchi, M.G., Martínez-Dopico, C., Drobe, M., Wemmer, K., Siegesmund, S., 2011, The Neoproterozoic-early Paleozoic metamorphic and magmatic evolution of the Eastern Sierras Pampeanas: an overview: *International Journal of Earth Sciences (Geologische Rundschau)*, 100, 465-488.
- Taylor, S.R., McLennan, S.M., 1981, The composition and evolution of the continental crust: Rare Earth element evidence from sedimentary rocks: *Philosophical Transactions of the Royal Society of London*, 301, 381-399.
- Taylor, S.R., McLennan, S.M., 1985, *The continental crust: its composition and evolution*: Oxford, United Kingdom, Blackwell Scientific Publications 312 p.
- Taylor, S.R., McLennan, S.M., 1995, The geochemical evolution of the continental crust: *Reviews of Geophysics*, 33, 241-265.
- Thomas, W., Astini, R., 2003, Ordovician accretion of the Argentine Precordillera terrane to Gondwana: a review: *Journal of South American Earth Sciences*, 16, 67-79.
- Toselli, A.J., 1990, Metamorfismo del ciclo Pampeano en el Noroeste Argentino, *in* Aceñolaza, F.G., Miller, H., Toselli, A.J. (eds.), *El Ciclo Pampeano en el Noroeste Argentino*, Serie Correlación Geológica: Tucumán, San Miguel de Tucumán, Argentina, Universidad Nacional de Tucumán, 4, 181-197.
- Toselli, A.J., Rossi de Toselli, J.N., Rapela, C.W., 1978, El basamento metamórfico de la Sierra de Quilmes, República Argentina: *Revista de la Asociación Geológica Argentina*, 33, 105-121.
- Toselli, A., Rossi de Toselli, J.N., 1983a, Metamorfismo de la Formación Puncoviscana en las provincias de Salta y Tucumán, Argentina, *in* V Congreso Latinoamericano de Geología, Buenos Aires, Argentina, 2, 37-52.
- Toselli, A., Rossi de Toselli, J. N., 1983b, Controles de metamorfismo y deformación en las parametamorfitas de las Cumbres de San Javier, Tucumán: *Revista de la Asociación Geológica Argentina*, 38, 137-147.
- Turner, J.C.M., 1960, Estratigrafía de la Sierra de Santa Victoria: *Academia Nacional de Ciencias de Córdoba, Argentina*, 49, 163-196.
- Verdecchia, S.O., Baldo, E.G., 2010, Geoquímica y procedencia de los metasedimentos ordovícicos del complejo metamórfico La Cebila, provincia de La Rioja, Argentina: *Revista de Ciencias Geológicas*, 27, 97-111.
- Willner, A.P., 1983, Evolución tectónica, *in* Aceñolaza, F.G., Miller, H., Toselli, A. (eds.), *La Geología de la Sierra de Ancasti*: Munich, Germany, Munster Forschungen zur Geologie und Paläontologie, 59, 157-187.
- Willner, A.P., 1990, División tectonometamórfica del basamento del noroeste Argentino, *in* Aceñolaza, F.G., Miller, H., Toselli, A.J. (eds.) *El Ciclo Pampeano en el Noroeste Argentino*: Serie Correlación Geológica: San Miguel de Tucumán, Argentina, Universidad Nacional de Tucumán, 4, 113-159.
- Willner, A.P., Miller, H., 1982, Polyphase metamorphism in the Sierra de Ancasti (Pampean Ranges, NW Argentina) and its relation to deformation, *in* V Congreso Latinoamericano de Geología: Buenos Aires, Argentina, Sociedad Geológica Argentina, 3, 441-455.
- Willner, A.P., Miller, H., 1985, Structural Division and Evolution of the lower Paleozoic Basement in the NW Argentine Andes: *Zentralblatt für Geologie und Paläontologie*, 1, 1245-1255.
- Willner, A.P., Miller, H., Jezek, P., 1985, Geochemical features of an Upper Precambrian-lower Cambrian greywacke/pelite sequence (Puncoviscana trough) from the basement of the NW-Argentine Andes: *Neues Jahrbuch für Geologie und Paleontologie*, 8, 498-512.
- Zimmermann, U., 2005, Provenance studies of very low to low-grade metasedimentary rocks of the Puncoviscana complex, northwest Argentina, *in* Vaughan, A.P.M., Leat, P.T., Pankhurst, R.J. (eds.), *Terrane processes at the margin of Gondwana*: London, United Kingdom, Special Publications of the Geological Society, London, 246, 381-416.

Manuscript received: June 23, 2012.

Corrected manuscript received: October 23, 2012.

Manuscript accepted: October 26, 2012.